

AD-A032 451

RICE UNIV HOUSTON TEX DEPT OF SPACE PHYSICS AND ASTRONOMY F/G 4/1
ATMOSPHERIC CONDUCTION CURRENT: OBSERVATIONS WITH A NEW METHOD --ETC(U)
SEP 75 H K BURKE

N00014-75-C-0139

NL

UNCLASSIFIED

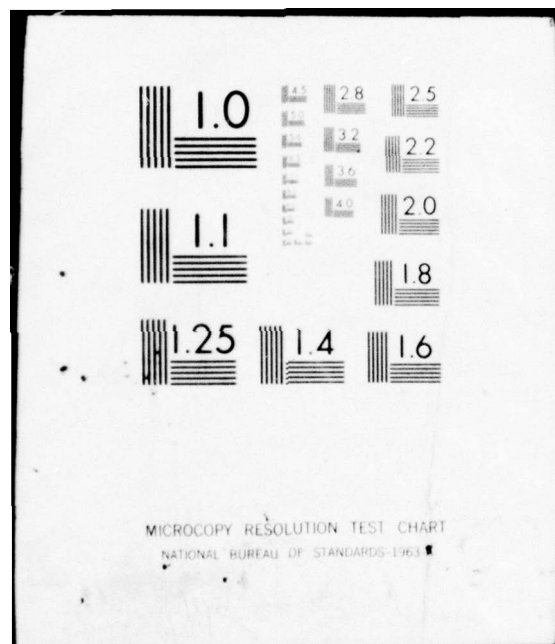
TR071-756

1 OF 1

AD A032451







AD A032451

One Copy Only
of complete text to TR071-756

P

REPORT DOCUMENTATION		READ INSTRUCTIONS BEFORE COMPLETING FORM	
1. REPORT NUMBER TR071-756	2. GOVT ACCESSION NO.	3. RECIPIENT'S CATALOG NUMBER	
4. TITLE (and Subtitle) ATMOSPHERIC CONDUCTION CURRENT: OBSERVATIONS WITH A NEW METHOD OF MEASUREMENTS.		5. TYPE OF REPORT & PERIOD COVERED Technical <i>rept.</i>	
7. AUTHOR(s) Hsiao-hua Kuo/Burke		6. PERFORMING ORG. REPORT NUMBER	
9. PERFORMING ORGANIZATION NAME AND ADDRESS Rice University P. O. Box 1892 Houston, Texas 77001		8. CONTRACT OR GRANT NUMBER(s) N00014-75-C-0139 N00014-67-A-0145-0004	
11. CONTROLLING OFFICE NAME AND ADDRESS Atmospheric Sciences Program, Code 465 Office of Naval Research Arlington, VA 22217		10. PROGRAM ELEMENT, PROJECT, TASK AREA & WORK UNIT NUMBERS NR211-191	
14. MONITORING AGENCY NAME & ADDRESS (if different from Controlling Office)		12. REPORT DATE 22 September 1975	
16. DISTRIBUTION STATEMENT (of this Report) Approved for public release; distribution unlimited.		13. NUMBER OF PAGES 7 (complete Thesis 92 pp.)	
17. DISTRIBUTION STATEMENT (of the abstract entered in Block 20, if different from Report)		15. SECURITY CLASS. (of this report)	
18. SUPPLEMENTARY NOTES Publication: M.S. Thesis, Rice Univ. Because of length of this thesis and limited quantities available, the technical report contains (1) title page, (2) table of contents, (3) abstract, and (4) acknowledgements sections only. The entire text can be obtained from National Technical Information Service.		16. DECLASSIFICATION/DOWNGRADING SCHEDULE	
19. KEY WORDS (Continue on reverse side if necessary and identify by block number) Springfield, VA 22151. Atmospheric Electricity, Air Conduction Current, Air Conductivity, Picoameters Measurements Techniques, Air Ions, Fog Prediction, Global Charge Balance.			
20. ABSTRACT (Continue on reverse side if necessary and identify by block number) A new device has been developed for measuring the atmospheric conduction current. This small portable instrument has a sensitivity of $.2\text{pA/m}^2$ and a range of 5pA/m^2 . 13 weeks of data acquired by this instrument are analyzed and several effects have been observed: (1) diurnal changes, (2) seasonal trends, (3) sunrise effects, (4) fog effects (anticipates visible fog formation and disappearance, (5) low cloud reversals, (6) thundercloud reversals, and (7) post-rain reversals. The data indicates that the theory of global charge balance should be re-examined.			

DD FORM 1473

1 JAN 73

EDITION OF 1 NOV 68 IS OBSOLETE

S/N 0102-014-6601

SECURITY CLASSIFICATION OF THIS PAGE (When Data Entered)

408798

VB

①

RICE UNIVERSITY
ATMOSPHERIC CONDUCTION CURRENT:
OBSERVATIONS WITH A NEW METHOD OF MEASUREMENT

by

Hsiao-hua Kuo Burke

A THESIS SUBMITTED
IN PARTIAL FULFILLMENT OF THE
REQUIREMENTS FOR THE DEGREE OF

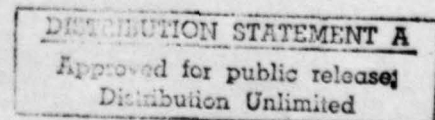
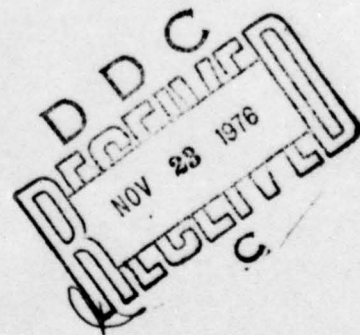
MASTER OF SCIENCE

Thesis Director's Signature:



Houston, Texas

September, 1974



Contents

Abstract

Chapter 1 The Global Atmospheric Electrical Circuit

I. Atmospheric Electric Field Intensity	1
II. Air Ions	1
III. Air-earth Conduction Current and the Balance of the Charge on the Earth	6

Chapter 2 Current Measurements

I. General Comments	9
II. Alternate Methods	17
III. Discussion of Measurement Techniques	25

Chapter 3 The Experiment

I. General Description	27
II. Theoretical Approach	29
III. Device Analysis	31

Chapter 4 Results

I. Preliminary Tests and Results	42
II. Outdoor Measurements	50
III. Conclusion and Modification of the Theory of Charge Balance	73
IV. Future Prospects	74

Appendix

Acknowledgements

References

A tilted rectangular stamp, likely from a library or archival collection. It contains several fields and checkboxes. At the top, there is a line for "ACQUISITION BY". Below this, there are checkboxes for "WIRE SECTION" (checked with a checkmark) and "BUT SECTION" (unchecked). Further down, there is a line for "BY" followed by "TO WHOM/WHICH DEPT". At the bottom, there is a large handwritten letter "A" in a box.

Atmospheric Conduction Current:
Observations with a New Method of Measurement

by

Hsiao-hua Kuo Burke

Abstract

Atmospheric electric field intensity, air conductivity, air-earth current density and air space charge density are the four closely related parameters of atmospheric electricity. The normal field intensity, about 130 volts/m near ground, decreases with altitude and also varies with cloud conditions and space charge concentrations. The conductivity of air, approximately $3 \times 10^{-14} \text{ ohm}^{-1} \text{ m}^{-1}$ near ground, increases with altitude and changes with aerosol content, humidity and other local conditions. The average conduction current density, on the other hand, stays more stable and is about 2 pA/m^2 for all altitudes. During fair-weather conditions, the directions of both the field and the current are downward from air to the ground (traditionally referred to as the positive direction).

Prior to our new method of measuring the atmospheric conduction current, there has been no direct measurement above ground. The instrument consists of an aluminum hemisphere pair suspended above the ground with the measuring electronics and the transmitter enclosed in the spherical structure. The upper hemisphere receives the positive component of the air-earth conduction current and the lower hemisphere the negative. The sum of the two is measured and the data are trans-

mitted to a recorder.

This is a direct and, therefore, more accurate method for measuring the air-earth current above the earth's surface. This method also avoids possible electrode effects and convection currents, which could not be distinguished from the conduction current, that are problems in the case of direct ground measurement. The electronic design employed here also includes compensation for the displacement current and temperature drifts. Experiments including testing Ohm's Law, the enhancement factor and effects of a mercury lamp light (UV- visible) were performed in the laboratory before detecting the air-earth conduction current.

The instrument reads current densities from -5 pA/m^2 to $+5 \text{ pA/m}^2$ with sensitivity up to 0.2 pA/m^2 . Data for 13 weeks were collected.

The results are divided into two categories: fair weather and disturbed weather conditions. Diurnal variations, seasonal trends, sunrise and fog effects are extensively discussed under fair weather conditions. During disturbed weather, the effects of low rain and thunder clouds are discussed. Observations indicate that charge separation occurs inside these clouds even when lightning activity is not observed. The charge concentrations within overcast clouds sufficient to reverse the normal atmospheric electric field direction are calculated. Negative current readings after rain and thunder storms are observed and discussed. From these results the air-earth charge balance theory is also modified.

This experiment shows that simultaneous measurements of field intensity, current density, conductivity and space charge density at

different locations are also required in order to draw more quantitative and accurate conclusions.

Chapter 1

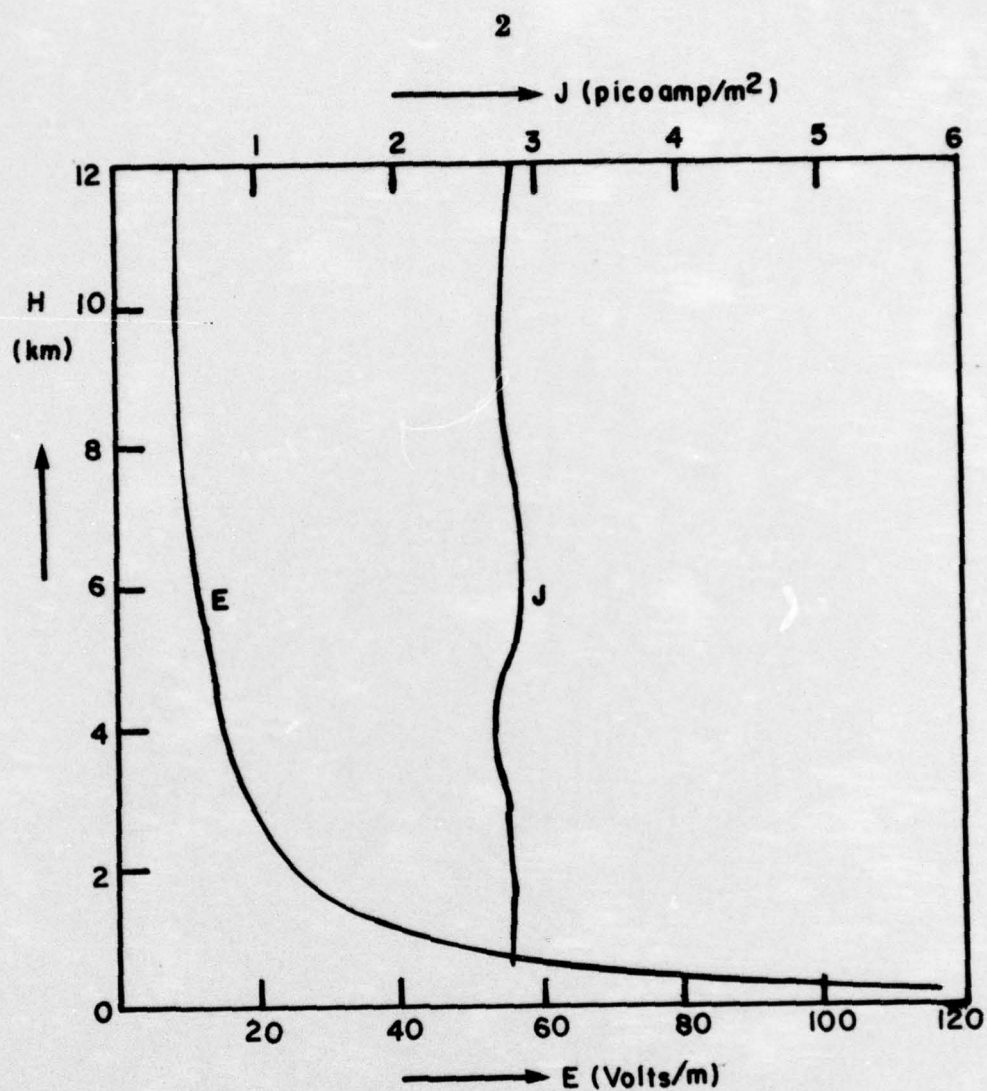
The Global Atmospheric Electrical Circuit

I. Atmospheric Electric Field Intensity

The statement "we are living in an intensive electric field" may sound unbelievable yet is very true. The magnitude of the average vertical field strength is about 130 volts per meter in our air in the downward direction. The field continues to exist but gets weaker as one goes up to higher altitudes (Figure 1.1). The total potential difference from the surface of the earth to the top of our atmosphere (~ 50 km, where the vertical gradient vanishes because of higher conductivity) is about 400,000 volts. The reason why there is nearly zero, instead of 200 volts, potential difference between a person's head and toes is because a human body is a relatively good conductor. Once in contact with the ground, the body and the ground become one equipotential surface.

II. Air Ions

Among the molecules and a wide range of particulates, there are ions that are also distributed with a wide range of sizes. For example, a molecule of oxygen can acquire or lose an electron and become a negative or positive ion. These ions usually accumulate with a few other molecules to form a cluster or attach themselves to particulates; in any event, they drift in the electric field.



Average Variation of E (Electric Field Intensity) and J (Conduction Current Density) with Height H up to 10 km

Figure 1-1 (Experimental values; from Israel, 1970)

At higher altitudes, ions are produced mainly by cosmic radiation. As a matter of fact, the investigation of the air ion source led to the discovery of the cosmic rays. Other ionization agencies are: (a) radiation from radioactive substances from soil and (b) radioactive gases produced by decay of (a). The so called "small ions" are these primary ions and they have a limited lifetime as small ions.

The situation near surface of the ground is usually somewhat different, Aerosols become charged as small ions rapidly attach themselves to these aerosols. They are bigger in size and are called "large ions". There also exist ions of sizes between small and large ions. They are called "intermediate ions". Table 1 gives the dimensions of the three different types of ions.

Type of Ions	Diameter
Large (Langevin)	$0.03\mu - 0.10\mu$
Intermediate	$0.003\mu - 0.03\mu$
Small	$0.001\mu - 0.003\mu$

Table 1. Size Range of Different Ions

Conductivity λ of the air, due to the drifting of ions, increases rapidly with altitude because:

- (1) ionization from cosmic rays becomes more effective at higher altitudes, and
- (2) the mobility of an ion increases when the neutral number density decreases. To prove this, we start from the relation

$$\lambda \propto \frac{\bar{v} \cdot l}{T}$$

where the parameters are

\bar{v} , the mean thermal velocity of the ion

l , the mean free path of the ions

T , the temperature of the air.

The increase of conductivity with respect to \bar{v} and l is obvious.

Conductivity also increases with the decrease of viscosity and in a gas viscosity increases proportionally with the temperature which implies the relationship of $\lambda \propto \frac{1}{T}$.

Since $l \propto 1/n$, n being the neutral number density, and $\bar{v} \propto \sqrt{T}$,

we get
$$\lambda \propto \frac{1}{n \sqrt{T}},$$

conductivity being inversely proportional to neutral number density.

Then from the relation

$$n \propto e^{-z/H}$$

where z being the altitude and H the scale height, we reach the conclusion that conductivity increases as we go higher.

(3) another factor which lowers the conductivity of air near ground

is the presence of numerous large aerosols. After small ions attach themselves to aerosols, their conductivity is decreased due to the increase of the collisional crosssectional area.

Mobility k of an ion in the air is related to the conductivity of the air. And conductivity is defined as

$$\lambda = (n_1 k_1 + n_2 k_2 + \dots) e$$

e : electric charge

for single charges, which is true for all but large aerosols. Also, mobility is inversely proportional to the cross-sectional area of the ion, or

$$k \propto \frac{1}{r^2}$$

r : radius of the ion.

Table 2 gives a brief idea of different properties of positive and negative small ions in the atmosphere at different altitudes:

Small Ions

Quantity	near ground	5 km	10 km	20 km	50 km
$(10^{-14} \text{ ohm}^{-1} \text{ m}^{-1})$	2.8	18	55	300	30,000
$n(+)$ (cm^{-3})	600	2000	3800	4400	
$n(-)$ (cm^{-3})	500	2000	3800	4400	
$k(+)$ ($\text{cm}^2/\text{sec}/\text{V}/\text{cm}$)	1.3	varies inversely with air density			
$k(-)$ ($\text{cm}^2/\text{sec}/\text{V}/\text{cm}$)	1.5				

Table 2. Atmospheric Electrical Quantities
(Allen, Astrophysical Quantities)

The given values of number densities near ground are true only under the condition of clean, clear air. For example, in the Boston vicinity, 700(+) and 500(-) ions per cm^3 on a clear pleasant day are reported. But on a dusty, rainy or foggy day, the measurements drop drastically down to 30 (+ or -) ions per cm^3 since the production rate of aerosols or droplets in these cases exceeds that of the generation of the

small ions.

III. Air-Earth Conduction Current and the Balance of the Charge on the Earth

The atmosphere has an electric field and, because of the presence of ions, the air becomes conducting. A current is constantly flowing down to the earth. This is called the air-earth conduction current. Although according to ion spectra, ions in the air are mostly intermediate and large ions, the air-earth conduction current is basically due to the existence of small ions. This current density is a few picoamperes per square meter and is fairly constant at all altitudes (Figure 1.1). Since from Section II the conductivity gets low near ground, the electric field is forced to increase near surface in order to conserve current.

The total conduction current flowing to the earth is about 1800 amperes which corresponds to a power of about 700 megawatts.

$$\begin{aligned} P &= I V = 1800 \text{ amp} \times 400,000 \text{ volts} \\ &= 7.2 \times 10^8 \text{ watts.} \end{aligned}$$

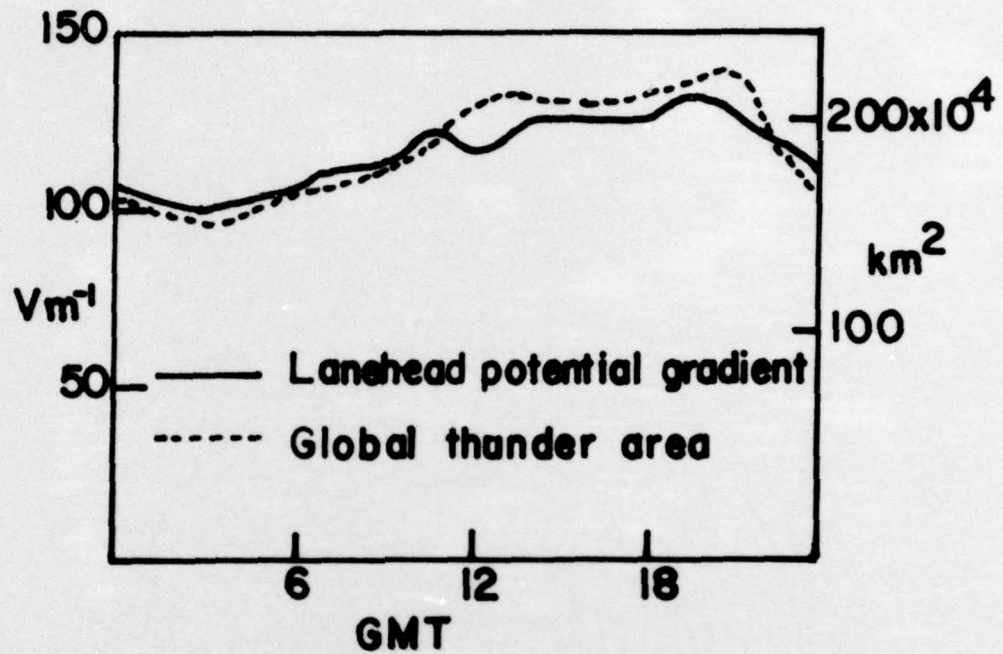
With this current coming down to the earth, however, the bound negative charge of the earth would be neutralized in a short period of time (Scrase, 1933) if not maintained by a source. Using the average values, we get:

$$\begin{aligned} \text{Surface charge density } \Delta &= \epsilon_0 E \\ &= 9 \times 10^{-12} \times 130 \text{ coul/m}^2. \end{aligned}$$

With current density $j = 10^{-12} \text{ amp/m}^2$, the time of neutralization

is about 20 minutes.

In other words, the negative charge of the earth would be discharged in less than half an hour. But we know the current keeps flowing down all the time, so there must be some other mechanism to balance the situation. After extensive research into the problem of electrical balance, the most likely mechanism for maintenance of the atmospheric potential is the thunderstorm and its lightning. Most lightning storms carry negative charges to the earth in large amounts for short periods of time, i.e. through lightning strokes. It is estimated that a good portion of 1800 amperes throughout the world is continuously being transferred by cloud to ground lightning activity. Figure 1.2 (Sharpless, et al., 1971) shows daily variations of potential gradient at Lanehead ($54^{\circ}46' \text{ N}$, $2^{\circ}15' \text{ W}$) and thunderstorm area on earth averaged between 1967 - 1969.



**Average Diurnal Variation of
Potential Gradient at Lanehead,
1967-69, and estimated area
of the Earth's Surface with
Active Thunderstorms**

Figure 1.2

Chapter 2

Current Measurements

I. General Comments

In the previous chapter an overview of the variations in atmospheric electrical parameters is presented. Because of variations of aerosol content in the air, conductivity near surface of the earth varies over a wide range at different locations and different times. Field intensities, responding to these changes, also have large variations. However, because of the continuity requirement, the current flowing down from higher altitudes to earth is comparatively more stable. This is one reason why it is more important to emphasize the air-earth current measurement in studies of the global electrical circuit.

It is a straight forward problem to demonstrate that it is the natural consequence for current density j to stay comparatively uniform at different altitudes while the electric field is forced to change. We assume as the initial conditions that E is uniform but j is discontinuous at some altitude and then follow the subsequent changes in the system.

In Figure 2.1 we assume an original uniform electric field of magnitude E_0 and draw an imaginary thin layer of negligible thickness. Charge will start residing on the layer if $j_1 \neq j_2$ where j_1 and j_2 are current densities above and below the layer. To get the electric field deduced from the charged layer, we use Gauss Law:

$$E = \frac{\rho}{\epsilon_0} \quad \text{or} \quad \frac{\partial(\nabla \cdot E)}{\partial t} = \frac{1}{\epsilon_0} \frac{\partial \rho}{\partial t}$$

and continuity equation

$$\nabla \cdot \mathbf{j} + \frac{\partial \rho}{\partial t} = 0,$$

thus

$$\frac{\partial (\nabla \cdot \mathbf{E})}{\partial t} = - \frac{1}{\epsilon_0} \nabla \cdot \mathbf{j}.$$

Integrate over volume of the slab, ,

$$\frac{\partial}{\partial t} \int_V (\nabla \cdot \mathbf{E}) d\tau = - \frac{1}{\epsilon_0} \int_V \nabla \cdot \mathbf{j} d\tau$$

or

$$\frac{\partial}{\partial t} (E_1 A_1 + E_2 A_2) = - \frac{1}{\epsilon_0} (-j_1 A_1 + j_2 A_2)$$

from Green's Theorem. $E_1 = E_2 = E$, $A_1 = A_2$ as described, we get

$$\frac{\partial E}{\partial t} = \frac{j_1 - j_2}{2 \epsilon_0} \quad (\epsilon_0 = 8.85 \times 10^{-12} \text{ farad/m}).$$

The change of E is about 100 volts/m every 30 minutes for every picoampere decrease from j_1 to j_2 . In other words, above the layer the E field will be decreasing at a rate of 100 volts/m every 30 minutes for one picoampere change of current density. And below the layer the field increases at the same rate. The electric field will approach zero above the layer thereby reducing j_1 while j_2 increases. The result is that on time scales of tens of minutes, j should be fairly constant.

After having established the stability of the air-earth conduction current, there are still several factors which require consideration when measuring the current. They are the following:

(1) Displacement Current

This is an effect or a condition due to the change of electric potential gradient with respect to time.

From surface charge density

$$\sigma = \epsilon_0 E,$$

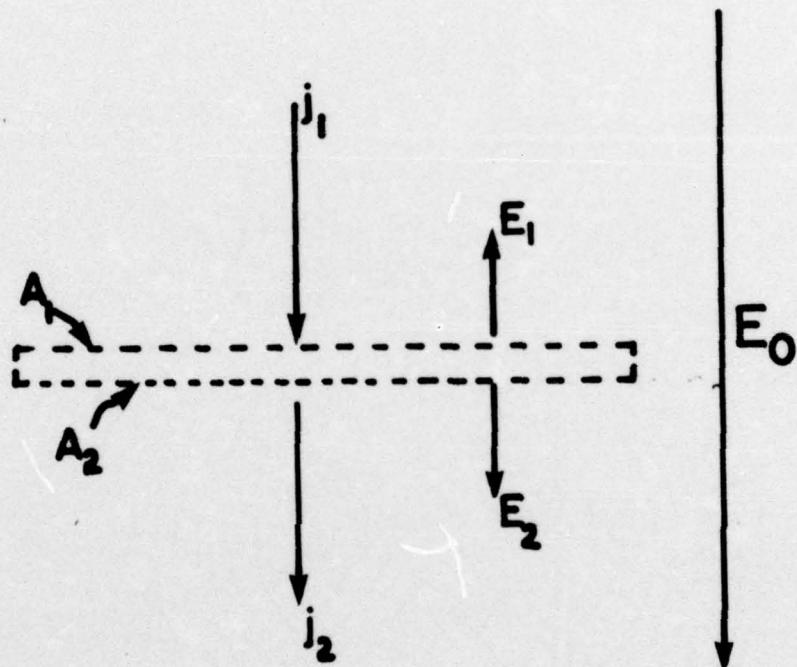


Figure 2.1

take derivative with respect to time:

$$\frac{d \sigma}{d t} = \epsilon_o \frac{d E}{d t}$$

or

$$j_{\text{displacement}} = \epsilon_o \frac{d E}{d t} .$$

This is not directly distinguishable from the true conduction current.

In other words, instantaneous measurement of the apparent current gives the sum of the displacement current and the conduction current.

Compensation for the displacement currents due to field changes must be arranged.

(2) Convection Current

There is a region in our lower atmosphere from earth surface up to about 3km called the Austausch (exchange) region in which there is periodic and fairly complete mixing of the air. If there are unbalanced or net space charges in the air, there exists a convection current which carries the surface air together with the ions, charged nuclei, etc. up to the top of the Austausch region.

Nolan and Nolan (1939, 1940) made measurements and concluded that there is very little convection current. However, Aspinall (1972), with more extensive observations showed that the magnitudes of conduction current and mechanical transfer current, which is due to space charge density and includes convection current, are about the same.

(3) Electrode Effect

The electrode effect is the nonuniformity of electrical conditions close to an electrode. Ions are created in pairs in the atmosphere by mechanisms described earlier. Thus, throughout most of the atmosphere

there are nearly equal numbers of positive and negative ions. However, near the surface of the earth the negative ions drift upward, and unless they are replaced by negative ions from radioactive substances in the ground they will leave a region of net positive charge near the surface.

Assume current density to be the same at different levels, or $j_g = j_f$, where the subscripts g and f refer to ground vicinity and free atmosphere, this implies

$$\lambda_g^+ E_g = (\lambda_f^+ + \lambda_f^-) E_f.$$

Assume also the conductivities of positive and negative ions remain the same below 100m, we have roughly

$$E_g = 2 E_f.$$

Calculation of the "Electrode Region":

Starting from the recombination equation

$$\frac{d n^+}{d t} = \frac{d n^-}{d t} = q - a n^+ n^-$$

n : number density of ions (cm^{-3})

q : new ion pairs produced per cm^3 per unit time ($\text{cm}^{-3} \text{sec}^{-1}$)

a : combination coefficient ($\text{cm}^3 \text{sec}^{-1}$).

Suppose $n^+ = n^-$, we can then write

$$\frac{d n}{d t} = q - a n^2.$$

When $\frac{d n}{d t} = 0$, we have $n_\infty = \sqrt{q/a}$ for equilibrium condition.

Solve the differential equation $\frac{d n}{d t} = q - a n^2$ under the assumption of equality of n^+ and n^- :

$$\int_{n_0}^{n_t} \frac{dn}{q - an^2} = \int_0^t dt$$

$$\frac{1}{2\sqrt{aq}} \ln \left| \frac{1 + \sqrt{a/q} n}{1 - \sqrt{a/q} n} \right| \Bigg|_{n_0}^{n_t} = t$$

$$\frac{1}{2\sqrt{aq}} \ln \left(\frac{n_\infty + n_t}{n_\infty - n_t} \cdot \frac{n_\infty - n_0}{n_\infty + n_0} \right) = t$$

$$\frac{n_\infty + n_t}{n_\infty - n_t} \cdot \frac{n_\infty - n_0}{n_\infty + n_0} = \exp(2\sqrt{aq} t)$$

Assume $\frac{n_\infty + n_0}{n_\infty - n_0} = B$, we get, after rearranging :

$$n_t = n_\infty \frac{B \exp(2\sqrt{aq} t) - 1}{B \exp(2\sqrt{aq} t) + 1}.$$

First approximation ($n_\infty \gg n_0$) gives

$$n_t = n_\infty \frac{\exp(2\sqrt{aq} t) - 1}{\exp(2\sqrt{aq} t) + 1}.$$

Substitution in typical atmospheric values

$$q = 10 \text{ cm}^{-3} \text{sec}^{-1},$$

$$a = 1.6 \times 10^{-6} \text{ cm}^3 \text{sec}^{-1},$$

we obtain equilibrium number density $n_\infty = \sqrt{q/a} = 2.5 \times 10^3 \text{ cm}^{-3}$.

In steady state condition, n_t reaches 95% Of the equilibrium value in time $t_{95\%}$ or

$$n_t = 0.95 n_\infty = n_\infty \frac{\exp(2\sqrt{aq} t) - 1}{\exp(2\sqrt{aq} t) + 1}$$

$$\exp(2\sqrt{aq} t) = 39$$

or

$$t_{95\%} = 460 \text{ sec.}$$

Assume field strength $E = 100 \text{ V/m}$ and mobility $k = 10^{-2} \text{ m/sec/100V/m}$, assume also the electrode region is below the region of 95% equilibrium. Negative ions can drift out of this region before equilibrium is reached. This gives the electrode region

$$D_E = K E t_{95\%}$$

to about less than 5m.

Now if we consider that large ions also exist in the air as is usually the case near ground, the range of electrode effect is appreciably shortened. Apply the "Linear recombination law" which is true in the case:

$$\frac{d n}{d t} = q - \beta n, \quad \beta = 2 \eta N$$

N : number density of large ions (cm^{-3})

η : recombination coefficient between small and large ions ($\text{cm}^3 \text{sec}^{-1}$).

Solve the differential equation for n :

$$\begin{aligned} \frac{1}{q} \int_{n_0}^{n_t} \frac{d n}{1 - (\beta/q) n} &= \int_0^t d t \\ - \frac{1}{q} \frac{q}{\beta} \ln \left(1 - \frac{\beta}{q} n \right) \Big|_{n_0}^{n_t} &= t \Big|_0^t \end{aligned}$$

$$\begin{aligned} \frac{1 - \frac{\beta}{q} n_t}{1 - \frac{\beta}{q} n_0} &= \exp (- \beta t) \\ n_t &= n_{\infty} \left[1 - \left(1 - \frac{n_0}{n_{\infty}} \right) \exp (- \beta t) \right] \end{aligned}$$

First approximation ($n_{\infty} \gg n_0$) gives

$$n_t = n_{\infty} [1 - \exp (- \beta t)]$$

Substitute in typical atmospheric values

$$q = 10 \text{ cm}^{-3} \text{ sec}^{-1},$$

$$N = 2500 \text{ cm}^{-3},$$

$$\eta = 10^{-5} \text{ cm}^3 \text{ sec}^{-1},$$

we get the equilibrium number density $n_{\infty} = \frac{q}{\beta} = 2 \times 10^2 \text{ cm}^{-3}$, and 95% of the equilibrium value n_{∞} will be reached when

$$n_t = 0.95 n_{\infty} = n_{\infty} [1 - \exp(-\beta t)]$$

$$\exp(-\beta t) = 0.05$$

or $t_{95\%} = 60 \text{ sec.}$

Assume the same E as in the previous case and a smaller k, electrode region must shrink down to a range of less than 1 m.

Hoppel (1969) made comparisons between theories of electrode effect and experimental observations of Crozier (1965), Gathman (1967) and Muhleison (1961). He reported that within the first quarter of a meter above ground there is a region of positive space charges which agrees with the prediction of the theory. But above that positive ions are balanced by an upward flow of negative ions from radioactive sources, such as Radon 220 and 222 in the soil near the surface. The reverse to normal electrode effect is sometimes observed on quiet nights due to the trapping of these radioactive ions. However, over the water or polar caps, radioactive gases are not expelled from the surface, and the electrode effect is observed to extend to higher altitudes.

(II) Different Methods of Measuring Air-Earth Current

The general methods of detecting atmospheric electric current have fallen into the following categories; (A) earth surface substitution, and (B) indirect method.

(A) Earth surface substitution:

The purpose of this method is to isolate a portion of the earth's surface and measure the charge reaching it in a given period of time. A plate is placed in the plane of the earth's surface and kept at the potential of the earth.

Some early investigations using this method included:

(1) Wilson (1908)

Wilson was the first one to take air-earth conduction current measurements from a collecting plate connected to an electrometer and a compensating condenser, which was used to compensate for the displacement current. The disadvantage is that it did not give continuous recordings.

(2) Simpson (1910)

Simpson adopted Wilson's method and corrected for the displacement current by measurements of the potential gradient at the start and end of each period.

(3) Kasemir (1955)

Kasemir compensated for the displacement current by using an R-C circuit in his measuring apparatus with the same time constant as the relaxation time of the air.

(4) Adamson (1960)

Adamson measured the current at one terminal of a differential amplifier and used a field machine to provide automatic and continuous compensation for the displacement current at the other terminal.

(5) Chalmers (1962)

Chalmers used an electronic amplifier to measure the charge collected on the plate during different time intervals. He got variations of current density, potential gradient and conductivity during different time intervals. He observed that the assumption of constant conductivity is incorrect which demonstrates the inadequacy of Kasemir's "matching circuit".

In short, direct methods with earth surface substitution can give accurate average readings at the surface when compensation is made for the displacement current. However, it can not distinguish the conduction current from convection current. In other words, we do not know how much convection current is involved. Furthermore, this method is confined to measurements at the ground and at the potential of earth surface. We can not adopt it to above-ground measurement nor can it be used over water.

Before proceeding to the indirect method, some trials of above ground measurements with raised wire or plate at local potential and at earth potential should also be mentioned:

(1) Raised wire net or plate at local potential

Israel and Dolezalek (1960) suggested a horizontal wire net or plate above earth ground and maintained at its natural potential in the atmosphere could be used as a plane of reference for observations of atmospheric electricity. However, the conduction current under such

conditions consists of a downward current carried by positive ions and an upward current carried by negative ions, and the two currents are nearly equal and the total current to the net of the plate is nearly zero. The proposal was soon abandoned.

(2) Raised wire at earth potential

Kasemir and Ruhncke (1958) suggested the measurement of the air-earth conduction current by an earthed wire at a height of one meter or more above the earth surface. The concentration of lines of current flow on the wire would enhance the conduction current relative to any convection current. It is proved as follows:

If the atmosphere at the height of the wire is at potential V in the absence of the wire, the wire carries a charge Q and the following relation holds:

$$V + Q/C = 0$$

where C is the capacitance of the wire. Since the wire is earthed, there can be nowhere by any positive charge on the wire when the surface charge on the earth is negative. The current density into the wire is then

$$j_w = \lambda^+ E_w = \frac{\lambda^+ C V}{A \epsilon_0}$$

since $E_w = -Q/\epsilon_0 A$ and $Q = -VC$. The current into the wire should be

$$I_w = \frac{\lambda^+ C V}{\epsilon_0}$$

or

$$\frac{I_w \epsilon_0}{C} = V \lambda^+.$$

The conduction current density is

$$j_{\text{cond}} = \lambda E$$

and the following relation is obtained:

$$j_{\text{cond}} = \lambda E = \lambda^+ V/h$$

$$= \frac{I_w \epsilon_0}{C h}$$

where h is the height of the wire. I_w and h are measured quantities, C can either be measured or derived theoretically. And since the wire is earthed, only λ^+ is involved.

The problems of this method are: (1) $\lambda \neq \lambda^+$ but $\lambda = \lambda^+ + \lambda^-$, total conductivity is the sum of conductivities of positive and negative ions, and (2) $E = V/h$ is not true since atmospheric electric field intensity is not independent of altitude.

(B) Indirect method

The indirect method of detecting the air-earth current consists of measuring: (a) the total conductivity of the air, and (b) the atmospheric electric field separately and simultaneously. Applying Ohm's Law, we get the current density:

$$j = \lambda_{\text{total}} E.$$

(a) Conductivity is determined by dissipation measurement or by aspiration method:

(1) Dissipation Measurement

This method adopts the idea that a charged conductor exposed to air containing ions suffers specific charge loss in the time which is proportional to the conductivity.

$$j^+ = \lambda^+ E = \frac{\lambda^+ Q^-}{4\pi\epsilon_0 r^2}$$

$$\text{or} \quad -\frac{dQ^-}{dt} = I^+ = j^+ A = \frac{4\pi r^2 \lambda^+ Q^-}{4\pi \epsilon_0 r^2} = \frac{\lambda^+ Q^-}{\epsilon_0}$$

$$\text{Similarly} \quad -\frac{dQ^+}{dt} = \frac{\lambda^- Q^+}{\epsilon_0}.$$

The restrictions of this method are: (1) only a minimum rate of air flow is permitted, and (2) the dissipation body must be well shielded from the atmospheric electric field. The two requirements are difficult to fulfill so it is not often used. Swan used this method for conductivity determination (1914, 1932).

(2) Aspiration Method

The air containing the ions is sucked through a plate or cylindrical capacitor with known electric field. The ion paths can be determined from the resultant of the two mutually perpendicular velocities: that of the air flow and the drift velocity due to the electric field. Current measurement in such a capacitor will then supply accurate data on the mobility and conductivity of air. Experiments using the aspiration method have been done by many people including Coroniti, Gunn, Hoppel and Whipple. Some work has recently been done at Rice University by J. Arnold (1974) and A. Few using aspiration method to construct the ion mobility spectrum which then serves as a monitor of air quality.

(b) Vertical potential gradient measurement

(1) The first type of method involves isolating an earthed surface such that there is no charge on it, then exposing it to the atmospheric electric field. The surface charge density on the

surface is proportional to the field strength E at the surface:

$$\sigma = \epsilon_0 E$$

or

$$E = \frac{\sigma}{\epsilon_0}$$

But this can only give the field strength at earth surface.

(2) Another type of method is to measure the potential difference between two horizontal levels at different heights. The potential is found through use of a "potential equalizer". A potential equalizer is a device such as a radioactive source by which a conductor can be brought to the same potential as the air in its neighborhood.

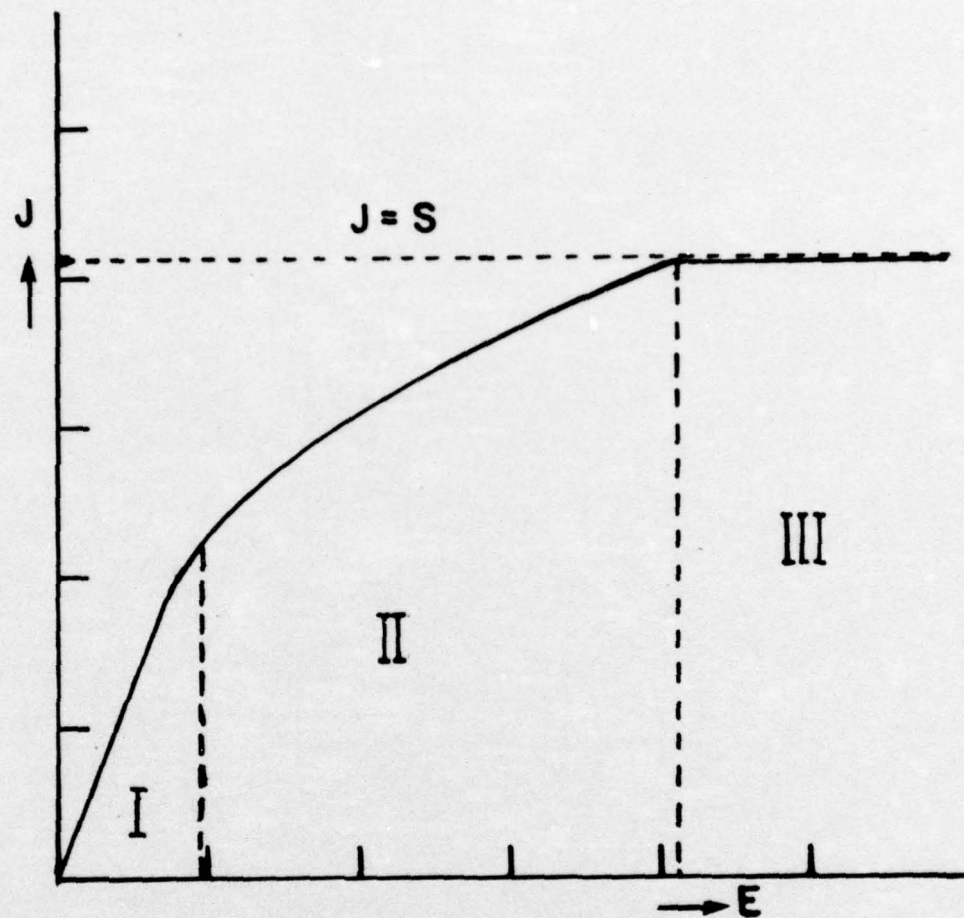
(3) Double field mills have also been used by people, such as Smiddy and Chalmers (1958), Ford (1958), Currie and Kreielsheimer (1960). The principal is to obtain continuous measurement of the air potential gradient close to ground using the bound charge from periodic shielding and unshielding of a conductor. Two field machines are placed on a conductor symmetrical with respect to a horizontal plane. The system behaves as an equalizer acquiring the potential of its surroundings; at the same time, the output from one half gives the potential gradient.

(4) W.D. Crozier (1963) brought the new idea of using passive antennas for atmospheric potential measurement. After any initial net charge on the antenna has leaked off, the antenna is at atmospheric potential and subsequently closely follows variations in the atmospheric potential. Antenna potential is sensed with an electrometer tube, coupled to an amplifier producing feedback for

neutralization input capacitance and for guarding. The RC time constant of the system is of the order of a few minutes which indicates good frequency response. The disadvantage of this arrangement is that it picks up static charges from blowing dust easily and as a result, is not good for use under windy conditions. Before any further comment, we should discuss Ohm's Law in more detail:

$J = \lambda E$ is valid only in a limited region. Figure 2.2 shows the current-voltage characteristics of conducting air. When an electric field is applied to a capacitor filled with conducting air, the current initially rise with the applied voltage according to Ohm's Law. This is valid as long as the current remains so weak that steady state conditions are not markedly disturbed by the field-induced ion drift. As the voltage increases, this loss will no longer be small compared with ion production, the current lags behind the Ohmic proportionality until, finally, field-induced ion removal and ion production completely compensate. When the voltage increases more, the current still remains constant.

So in order to get real current values from the indirect method, λ must be measured in a device that produces a field strength E that has the same field strength of the system under evaluation. This is sometimes difficult to achieve. For example, when doing the measurements at a higher altitude in an aircraft, the electric field strength can be as low as one volt per meter. However, it is not easy to get ion mobility measurements from the aspiration



I: Domain of Ohmic Current

II: Domain of Unsaturated Current

III: Domain of Saturated Current

**Current Voltage Characteristic of
an Ionized Gas**

Figure 2-2 (from Israel; 1970)

method with the applied field strength at the same magnitude.

Also, the process of sampling the air to measure λ must not alter the native undisturbed value for λ and the measured electric field strength must be converted to the true undisturbed value for E with precision.

III. Discussion of Measurement Techniques

From the previous sections, we realize that the air-earth current density stays more stable than the other parameters of the global electrical circuit. As a result, it is the best parameter to measure in order to understand the whole atmospheric electric behavior.

Also, from the brief review above, we realize that air-earth current measurements at or very close to earth surface are less meaningful because of the complications introduced by the electrode effect and the convection currents. Furthermore, if we want to measure the electric current above ground, the earth surface substitution is not applicable and the indirect method is not accurate due to the reasons just described. Therefore, a new method of above ground current measurement is needed at this point. In 1962, Chalmers made the following suggestion: "If two horizontal plates are separated by a thin layer of insulating material and put at the potential of their surroundings, then the upper plate will receive, in the normal weather field, the positive component

of the conduction current and the lower plate the negative component.... These could be added together to give the total current." The experiment presented in this thesis adopted the original Chalmer's idea with other innovations.

Chapter 3

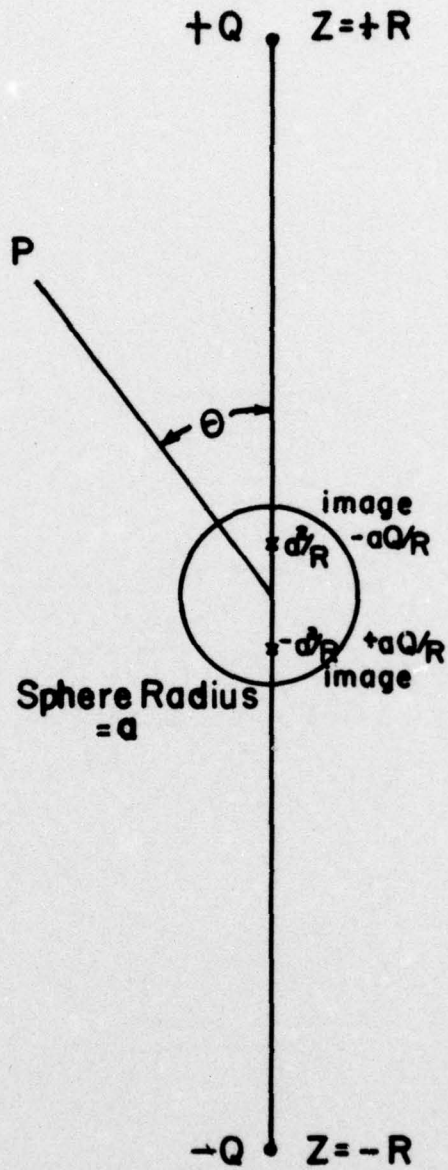
The Experiment

I. General Description

In this experiment, two six-inch radius hollow aluminum hemispheres are attached together with a horizontal insulating disk in between. The sphere is used as a probe to investigate the atmospheric conduction current in the laboratory and in the air near the ground. The hemisphere pair is supported above the earth by strings attached between the insulating disk and an insulated 9 ft. high, 20 ft. wide tri-leg wood frame. Thus the sphere will, after any net charge has leaked off, assume the potential of the air surrounding the sphere and can make the atmospheric current measurement in the air above the surface.

Some advantages of the instrument are:

- (1) This is a direct measurement of air-earth current and is capable of giving more accurate results of the air-earth conduction current.
- (2) Convective current in this case is negligible since the dimension of the sphere is smaller than the scale over which space charge density changes noticeably.
- (3) Displacement current is compensated by the RC network which will be described later. The RC time constant in this experiment is about 2000sec. which is in the same order of magnitude as the atmospheric "relaxation time".
- (4) Measurement can be taken above earth's surface, thereby avoiding



Conducting Sphere in a Uniform Electric Field

Figure 3.1

the electrode region irregularities if they are present.

(5) The whole device is small and portable. Furthermore, due to the spherical geometry, the electronic circuit as well as the power supply can be enclosed within the device which reduces extraneous noises. And at the same time, it is protected from rain and moisture which can damage the electronics.

II. Theoretical Approach

The sphere assumes the potential of the air that surrounds it. The geometrical enhancement of the electric field due to the spherical conductor is calculated below:

Figure 3.1 shows a conducting sphere in a uniform electric field. We apply the image method (Jackson, 1969) to this system.

Potential Φ at point P will be that due to the charges $^+ Q$ at $z = ^+ R$ and their images $^- Q \frac{a}{R}$ at $z = ^- \frac{a^2}{R}$ as illustrated in Figure 2.1.

$$\Phi = \frac{1}{4\pi\epsilon_0} \left[- \frac{Q}{\sqrt{r^2 + R^2 + 2rR \cos\theta}} + \frac{Q}{\sqrt{r^2 + R^2 - 2rR \cos\theta}} + \frac{\frac{aQ}{R^2}}{\sqrt{r^2 + \frac{a^2}{R^2} + \frac{2a^2 r}{R} \cos\theta}} - \frac{\frac{aQ}{R^2}}{\sqrt{r^2 + \frac{a^2}{R^2} - \frac{2a^2 r}{R} \cos\theta}} \right]$$

Assume $R \gg r$ which is equivalent to assuming a uniform external field:

$$= - \frac{1}{4\pi\epsilon_0} \left\{ \frac{Q}{R} \left\{ \left(1 + \frac{2r}{R} \cos\theta \right)^{-\frac{1}{2}} - \left(1 - \frac{2r}{R} \cos\theta \right)^{-\frac{1}{2}} \right\} + \frac{aQ}{R} \left\{ \left(1 + \frac{2a^2}{Rr} \cos\theta \right)^{-\frac{1}{2}} - \left(1 - \frac{2a^2}{Rr} \cos\theta \right)^{-\frac{1}{2}} \right\} \right\}$$

$$= -\frac{1}{4\pi\epsilon_0} \left\{ -\frac{Q}{R} \frac{2r}{R} \cos\theta + \frac{a}{r} \frac{Q}{R} \frac{2a^2}{Rr} \cos\theta \right\}$$

$$= \frac{1}{4\pi\epsilon_0} \left(\frac{2Q}{R^2} \right) \left[r - \frac{a^3}{r^2} \right] \cos\theta.$$

But the applied field $E_0 = \frac{1}{4\pi\epsilon_0} \frac{2Q}{R^2}$, this gives

$$\Phi = E_0 \left[r - \frac{a^3}{r^2} \right] \cos\theta.$$

where the second term refers to the induced surface charge.

$$\vec{E} = -\vec{\nabla}\Phi$$

$$\therefore \vec{E} = -E_0 \left\{ \left(1 + \frac{2a^3}{r^3}\right) \cos\theta \hat{r} - \left(1 - \frac{a^3}{r^3}\right) \sin\theta \hat{\theta} \right\}.$$

We can look at several limiting cases now:

$$\vec{E}_{\theta=0} = -E_0 \left(1 + \frac{2a^3}{r^3}\right) \hat{r} \text{ and}$$

$$\vec{E}_{\text{surface of the sphere}} = -E_0 3\cos\theta \hat{r}.$$

Induced surface charge density

$$\sigma = -\epsilon_0 \frac{\partial\Phi}{\partial r} \Big|_{r=a} = -\epsilon_0 E_0 3\cos\theta.$$

And

$$j_{\text{surface}} = 3\lambda E_0 \cos\theta.$$

Current flowing on the top hemisphere is

$$I_{\text{top}} = \int j_{\text{surface}} dA$$

$$= 3\lambda^+ E_0 a^2 \int_0^{\pi/2} \int_0^{2\pi} \cos\theta \sin\theta d\theta d\phi$$

$$= 3\lambda^+ \pi a^2 E_0.$$

or

$$I_{\text{bottom}} = 3\lambda^- \pi a^2 E_0$$

such that

$$I_{\text{through the circuit}} = 3 \left(\frac{\lambda^+ + \lambda^-}{2} \right) \pi a^2 E_0 = \frac{3}{2} \lambda_{\text{total}} \pi a^2 E_0.$$

The corresponding current density in the air should be

$$j = \lambda_{\text{total}} E_0 = \frac{I}{3\pi a^2} \cdot 2$$

In other words, we are measuring only half of the true air-earth conduction current. This is the same problem encountered when doing the measurement with a grounded plate except in the latter case the electrode effect will double the original field in the ideal condition and make up for the current density measured. But in our case, it can be shown that the field change due to electrode effect is much smaller than the original atmospheric electric field. (**For proof, see the end of the Chapter, p.40-1.)

III. Device Analysis

The hemisphere pair, as described earlier, are connected together with a teflon disk in between and is suspended in the air by horizontal teflon coated wire attached to the insulated wood frame.

Inside the sphere there are:

- (1) Battery power supply and voltage regulator,
- (2) Electronics section which includes
 - (a) Preamplifier,

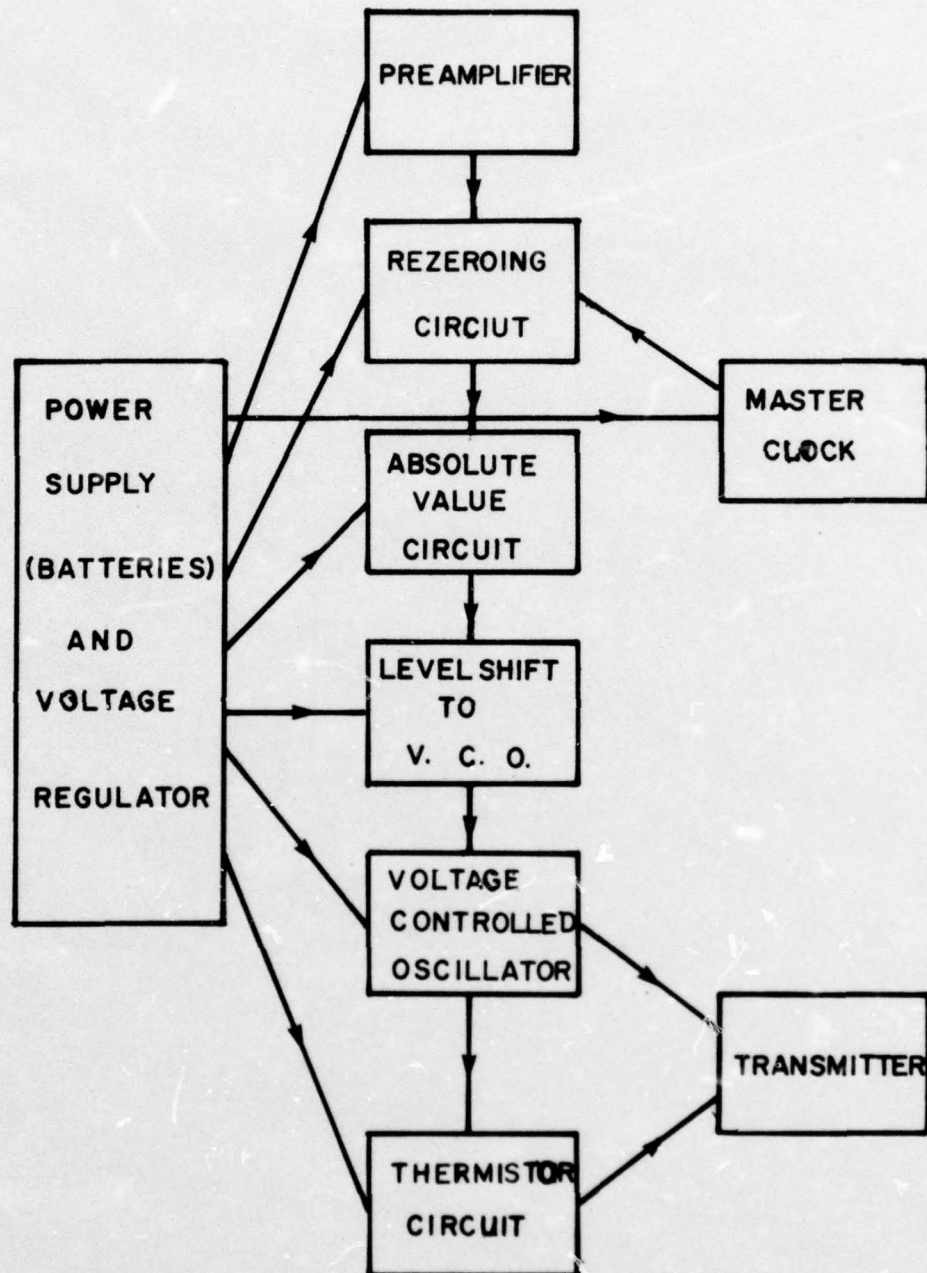


Figure 3.2

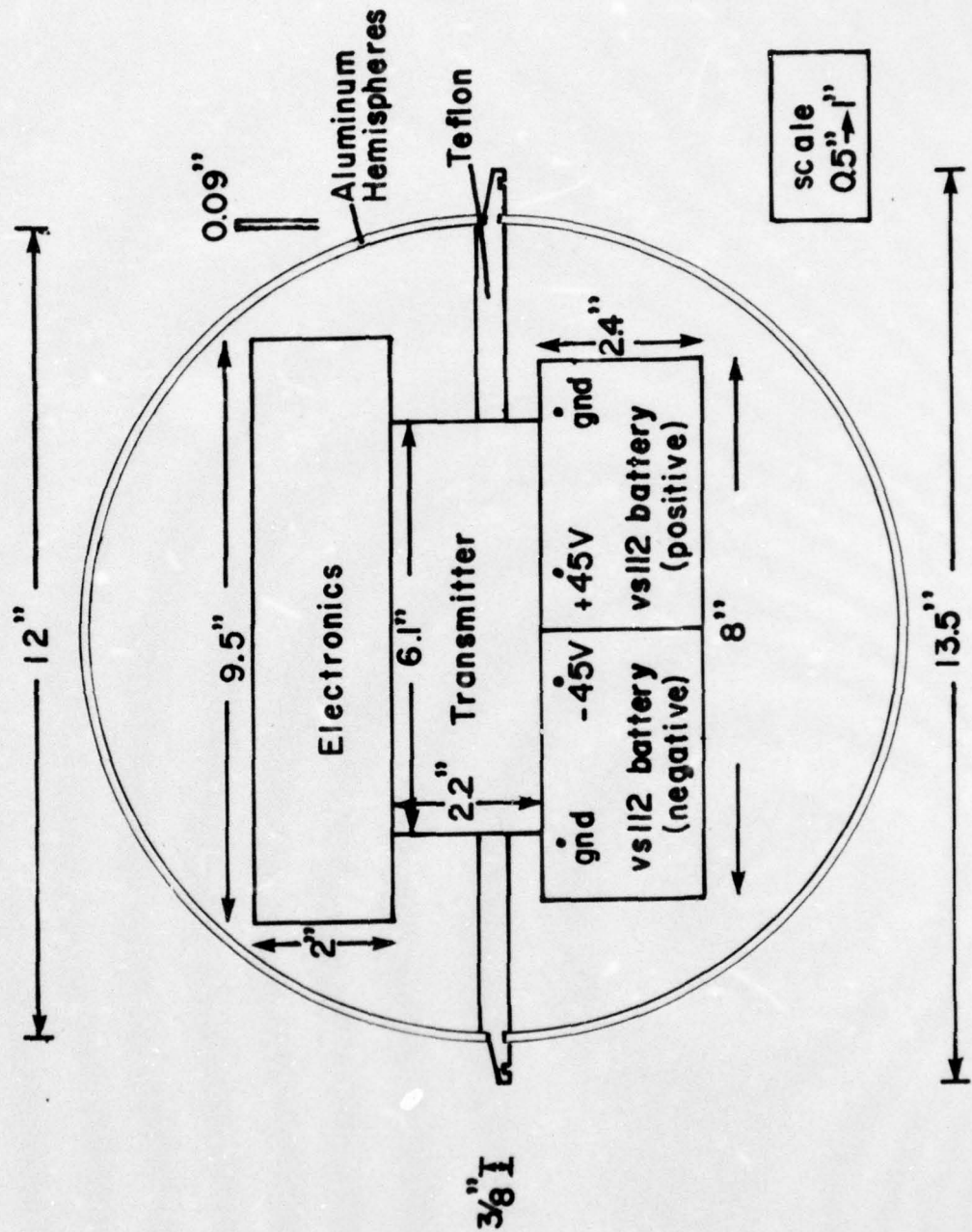


Figure 33

- (b) Rezeroing circuit with master clock,
- (c) Absolute value circuit,
- (d) Voltage controlled oscillator, and
- (e) Thermistor circuit

(3) Transmitter

as shown in the schematic diagram (Figure 3.2). They fit in the sphere as shown in Figure 3.3.

The electronic circuit must meet two criteria. First, it has to be sensitive enough to measure the small conduction current from the air. Secondly it also has to be stable through the measurements so that long term readings can be taken.

The Model 311J electrometer (manufactured by Analog Devices) amplifier is capable of meeting these goals. It is an ultra low bias current varactor bridge operational amplifier with extremely low input bias current (± 10 fA) ($\text{fA} = 10^{-15}$ Amp) and high input impedance (10^{14} ohms). The sufficient gain coupled with ultra-low offset of the amplifier makes currents of the order of 10^{-14} ampere detectable. An input impedance of 10^{10} ohms per channel for the RC circuit in front of the amplifiers was chosen as the near optimal value in terms of temperature drift of the amplifier. With this value fixed, the input capacitance of 10^{-7} farad acts to suppress transient currents on the input to the device from movement, noise, etc. of the sphere.

Several tests of the preamplifier characteristics were performed to verify the manufacturer's specifications. The offset (± 10 fA), sensitivity, and linearity of the preamplifier were evaluated with

a Keithley 261 picoampere source. The effect of the long term drift was also tested. It did not exceed ± 20 fA for zero input for a period of a day. The test of accuracy of the input impedance of the RC circuit was performed with an Ohmmeter (Keithley 600A Electrometer, full range for resistance measurement is 10^{14} ohms); measurements both with and without the hemispheres were made. Both showed the same effective resistance of 10^{10} ohms. Also the resistance between the two hemispheres with the teflon disk in between and the internal circuit disconnected was found to be out of range of the ohmmeter, which indicates a resistance exceeding 10^{13} ohms.

The pair of 311J's are utilized in a push-push configuration for the gain set (sensitivity = 1 fA/volt) and the possibility of offsetting drifts between the two amplifiers.

The RC time constant in this case is

$$\begin{aligned}\tau &= R C \\ &= 10^{10} \times 2 \text{ ohms} \times 10^{-7} \text{ farad} \\ &= 2000 \text{ sec.}\end{aligned}$$

To explain how the RC network compensates the possible displacement current, we consider an imaginary cube of air with conductivity λ , its effective resistance is then $\frac{d}{\lambda A}$. It can also be considered as though there were conducting plates on two opposite faces which implies an effective capacitance of $\frac{\epsilon_0 A}{d}$. The time constant RC for the system is $\frac{d}{\lambda A} \cdot \frac{\epsilon_0 A}{d} = \frac{\epsilon_0}{\lambda} = \frac{8.85 \times 10^{-12} \text{ farad m}^{-1}}{3 \times 10^{-14} \text{ ohm}^{-1} \text{ m}^{-1}} \approx 200 \text{ sec}$ which is less than the RC value of our circuit. The total current density to the collector is:

$$\begin{aligned} j_{\text{total}} &= j_{\text{cond}} + j_{\text{disp}} \\ &= j_{\text{cond}} + \epsilon_0 \frac{dE}{dt} \end{aligned}$$

Consider a fluctuating electric field $E = E_0 e^{\omega t}$. The voltage drop V across the RC circuit can be expressed in terms of the impedance X as

$$\begin{aligned} V &= |X| 3A \left(j_{\text{cond}} + \epsilon_0 \frac{dE}{dt} \right) \\ &= \frac{R}{1 + R^2 C^2 \omega^2} 3A (\lambda E_0 + \epsilon_0 E_0 \omega) \end{aligned}$$

For $\omega \ll \frac{1}{RC}$ and since $RC \geq \frac{\epsilon_0}{\lambda}$, $\omega \ll \frac{\lambda}{\epsilon_0}$

$$V \approx R 3A \lambda E_0 = 3RAJ_{\text{cond.}}$$

This means in our case for slow fluctuations of the electric field, the displacement current effect is negligible.

The rezeroing circuit is designed to compensate for long-term drift. An analog memory is used to sample the output of the preamplifier during ambient conditions. It is achieved by a circuit between the preamplifier and the signal source, the hemispheres. At the end of every fixed time interval, prescribed by the master clock circuit, the preamplifier input is disconnected from the signal (RL2 opens in Figure 3.4) and, when the preamplifier is stabilized, its output is recorded in the memory (RL1 closes in Figure 3.4). The principle of this technique lies in the linearity of the amplifier. For we know that:

$$S_0 = (S_1 - S_a) A$$

where S_0 is the output signal voltage, S_1 is the input signal voltage, S_a is the offset of the amplifier and A is its gain. Let V_R be the voltage recorded in the memory, we get:

$$\begin{aligned} V_R &= (0 - S_a) A \\ &= -S_a A. \end{aligned}$$

RL1 then opens up and RL2 closes to receive signals from outside source again. The operation is completed through a unity gain amplifier which provides the output voltage V_o :

$$\begin{aligned} V_o &= S_o - V_R \\ &= (S_1 - S_a) A - (-S_a A) \\ &= S_1 A. \end{aligned}$$

In other words, V_o is directly proportional to S_1 , the differential voltage induced between the two hemispheres. Thus, the rezeroing circuit, compensates for any long term drift in the preamplifier. The circuit diagram of the preamplifier and the rezeroing section is shown in Figure 3.4.

Following the rezeroing circuit is an absolute value circuit with unity gain. It has two outputs. One is simply proportional to the magnitude of the input. The other output is a logic signal to indicate when the output has a different polarity from the input. Hence for a negative value input, the output triggers an oscillation of about 10 Hz which indicates a negative polarity.

Between the absolute value circuit and the voltage controlled oscillator, there is a level shift circuit. This is necessary because the absolute value circuit is referenced to ground, but the voltage-to-frequency converter expects an input referenced to a 8.3 V power supply. The operation of the circuit is to invert every V_o volts from the absolute value circuit to $(8.3 - |V_o|)$ volts to the voltage-to-frequency converter.

The signal representing the incoming voltage is then an oscillator with frequency modulation. Its output F is then a signal with frequency directly proportional to $|V_o|$ which is presented as $8.3 - |V_o|$. In other words,

$$F (8.3 - |V_o|) = K_o |V_o|$$

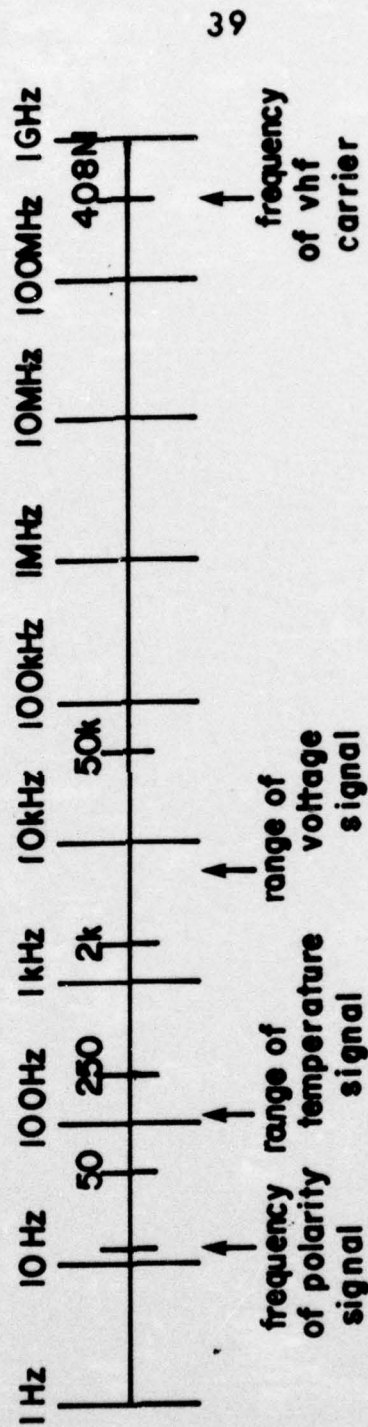
where K_o is a constant, set through an internal adjustment to 14.3 kc/V.

This signal chain also includes another reference operation. When the rezeroing system is locking its memory onto the offset of the preamplifier, a reference voltage of one volt is fed into the level shift input, whence a frequency $F = K_o \cdot 1$ volt is transmitted, thus evaluating the constant K_o during each cycle.

The temperature drift of the entire circuitry was tested in a closed chamber. The result showed it did not exceed 500 ppm (part per million).

Through the thermistor circuit the temperature is converted to voltage and then to a frequency modulated oscillation by a voltage-to-frequency converter. Since the electronics has an optimum temperature range of operation, the thermistor circuit serves the purpose that excess of this optimum temperature range inside the sphere can be detected.

The three f.m. signals: (1) from the thermistor output, (2) from the voltage controlled oscillator and (3) from the polarity indicator of the input are combined together (see Figure 3.5 of different frequency domains) are fed to the base junctions of a pair of vhf signal they generate, which is transmitted through a half-wavelength loop antenna located in the sphere. The frequency of operation is approximately 408 megahertz. The length of the loop antenna is



The Frequency Domain as Employed

Figure 3-5

$$l = \lambda/2 = \frac{1}{2} \frac{3 \times 10^8 \text{ m sec}^{-1}}{408 \times 10^6 \text{ sec}} = 0.368 \text{ m.}$$

Out side the sphere, the signal travels through

- (1) Receiving antenna,
- (2) Receiver,
- (3) Receiving filter,
- (4) Chart recorder, which reads the current output and indicates the polarity, and
- (5) Frequency counter which reads the temperature output.

The systematic diagram is shown in Figure 3.6.

The receiving antenna is attached to the support frame for the sphere at a distance of several meters from the sphere. The cable from the antenna is then routed into the building where the receiving station is located. And from the filter output through a frequency-to-voltage converter, the data are finally presented on the chart recorder and the frequency counter.

**Brief calculation of ΔE , the electric field change due to the electrode effect around the sphere:

Maximum height h of the electrode layer is given by the distance traveled by small ions while air passes over the sphere,

$$h = \pi a \frac{v}{u}$$

where u is the flow velocity of air around the sphere and v is the drift velocity due to the mobility of ions, $v = k_{av} E_0$.

The mean reaction time of ions in the electrode region is given by

$$\tau = \frac{\pi a}{u}$$

The volume involved outside each hemisphere is $V = 2\pi a^2 h$ and the external charge reached in the region in time τ is $\frac{I \tau}{2}$.

This implies the equivalent surface charge density on the metallic surface due to the space charge built up from the absence of ions ($\frac{1}{2}$ of I) leaving the metallic surface is

$$\begin{aligned} \sigma &= \frac{I \tau}{2 V} \pi a \\ &= \frac{I \frac{\pi a}{u}}{4 \pi a^2 h} \quad a = \frac{j}{4 k E_0} \pi a \end{aligned}$$

or

$$\begin{aligned} E &= \sigma / \epsilon_0 \\ &= \frac{j \pi a}{4 k E_0 \epsilon_0} \end{aligned}$$

For standard atmospheric values, $j = 2 \times 10^{-12}$ amp/m², $k = 1.3 \times 10^{-4}$ m² sec⁻¹ volt⁻¹ and $E_0 = 130$ volts/m, we get $\Delta E \doteq 1$ volt /m which is negligible compared to the normal atmospheric field.

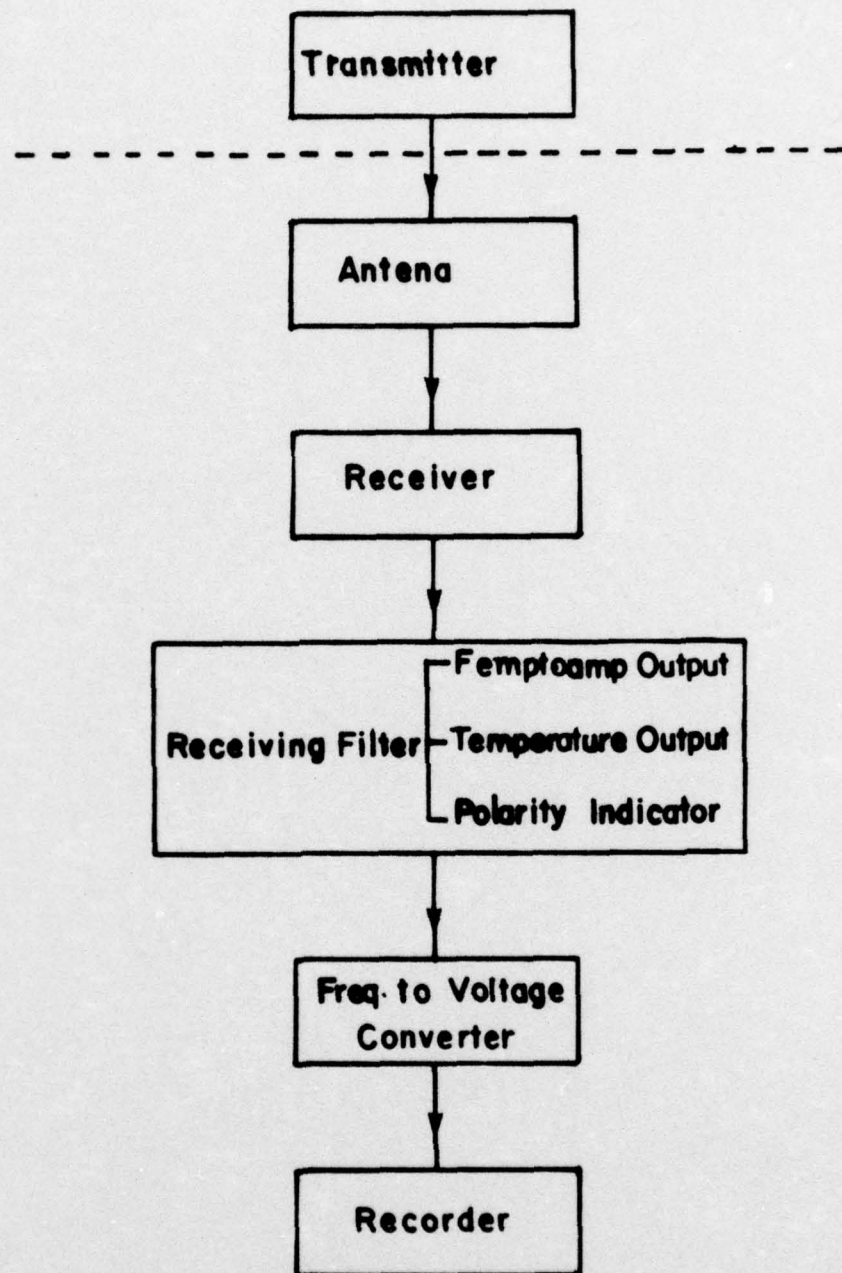


Figure 3.6

Chapter 4

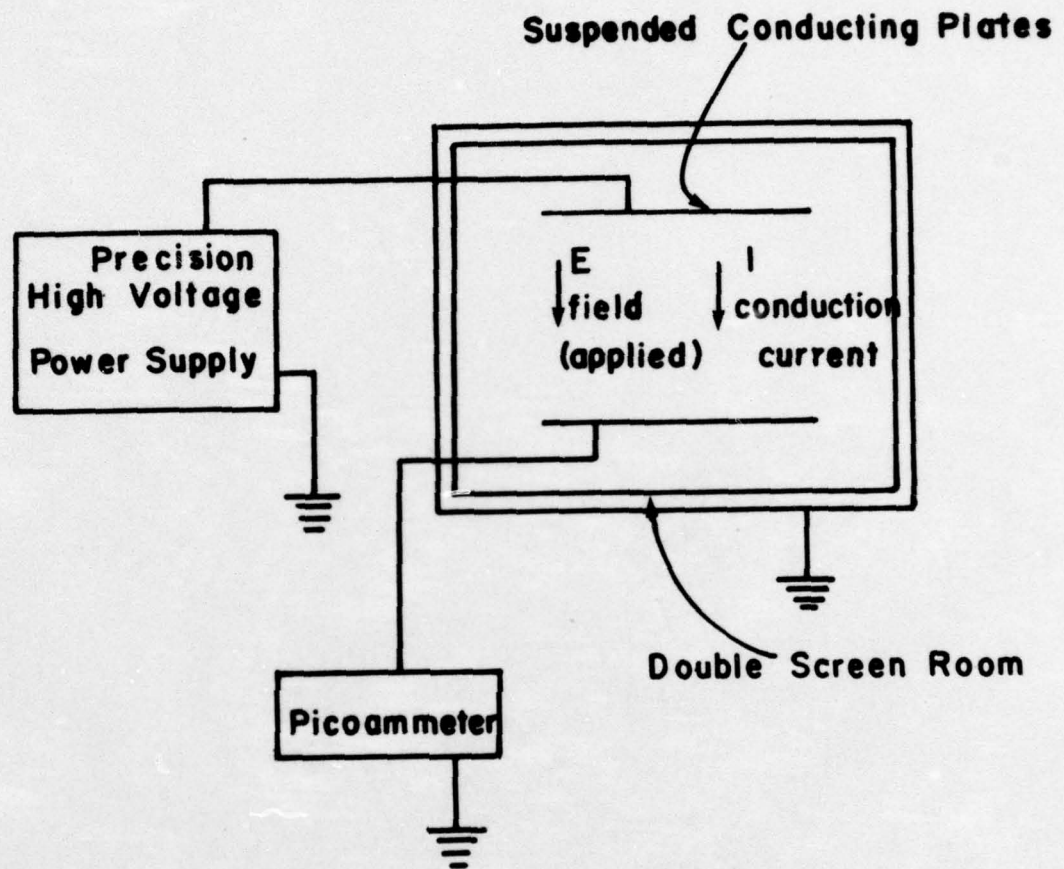
Results

I. Preliminary Tests and Results

Before detecting the air-earth current in the atmosphere, several laboratory experiments were performed to verify the performance of the instrument. Two parallel conducting plates (6' x 6' each) were supported horizontally in a double screen room (10' x 10' x 8') whose function was to shield off the extraneous electric fields. The separation between the plates can be adjusted. Various voltages were applied between the plates and the magnitude of the air conduction current flowing between the plates was measured. Furthermore, the effect on the increased current reading was obtained by using a mercury lamp. Also, by suspending the hemisphere pair current detector between the parallel plates, we compared the parallel plates reading with the sphere reading in the screen room.

(1) Current flowing between parallel plates:

The schematic diagram for this experiment is shown in Figure 4.1. An electric field is applied between the plates. Applied field intensities vary from zero to ten thousand volts per meter and conduction current readings are taken from the picoammeter. A typical result is shown in Figure 4.2. A near-linear relationship between the current and the electric field intensity (i.e. the slope on the log-log plot is close to one) is observed in the lower range--supposedly the Ohmic region. This shows that Ohm's Law is only an



Arrangement for Detecting Current in
the Screen Room from Applied E Field

Figure 4.1

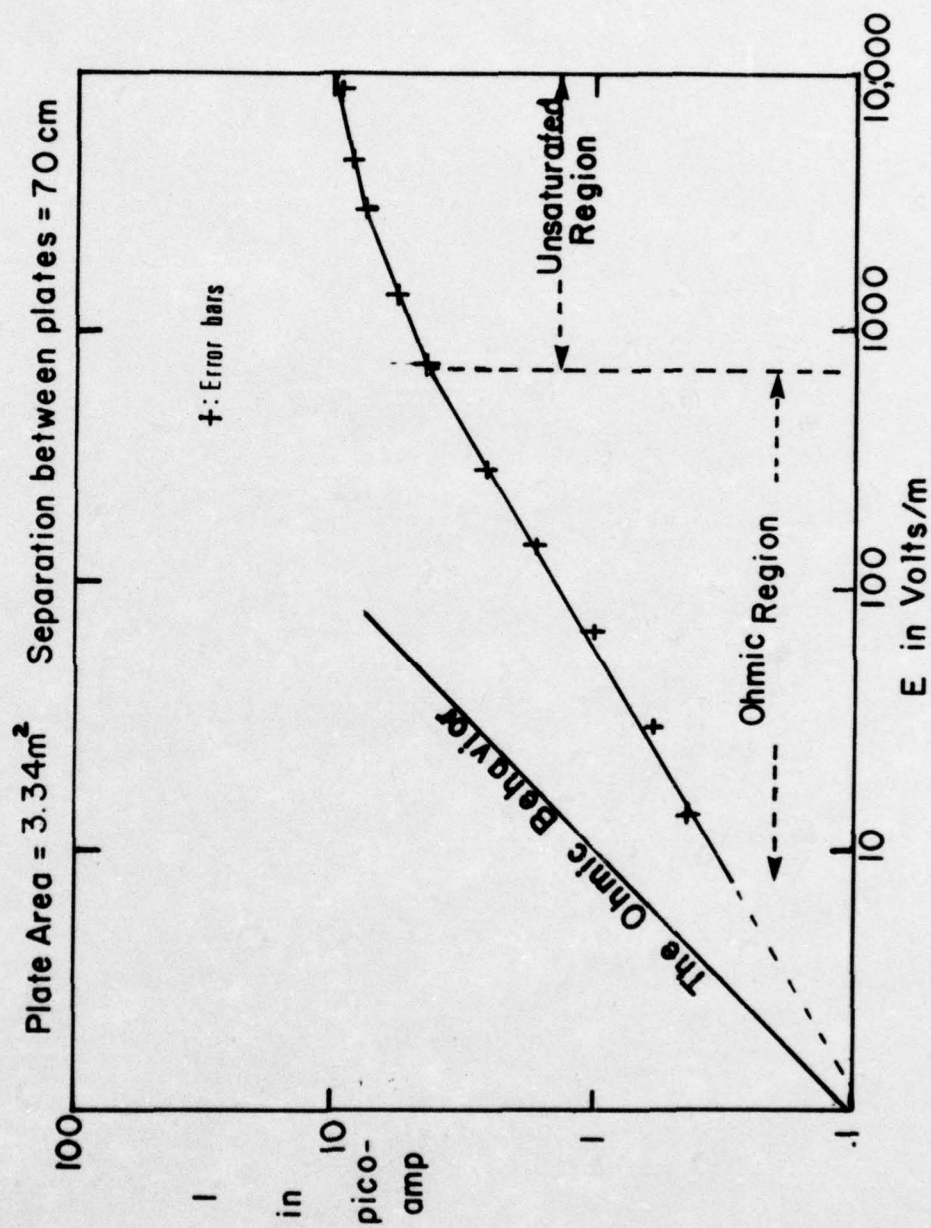


Figure 4.2

approximation to actual behavior in normal air (the lower range of this experiment). The slope of I/E flattens as the field strength increases which designates the unsaturated region.

The explanation is as follows: The current initially rises with the applied voltage linearly. This is valid as long as the current remains so weak that the steady state conditions which occur in the absence of a field are not markedly disturbed by the field-induced ion drift. If this loss is no longer small in comparison with the ion production, increasing the voltage will cause the current to lag behind the Ohmic proportionality until finally, field-induced ion removal and ion production completely compensate. They are called unsaturated and saturated regions respectively.

(ii) Increased air conduction readings in presence of a mercury lamp:

A mercury lamp whose spectrum ranges from ultra-violet to visible light (2500\AA - 7000\AA) is used for the experiment. A beam of light from the lamp optics is passed through a set of choppers to control the amount of light passing through the air between the plates.

Increased air conduction current due to the presence of the photons is observed. Results show the distinct effect of the UV-visible light on increasing the conductivity of the air. Figure 4.3 is an example.

The energy involved in a stream of photons (a beam of electromagnetic radiation) of wavelength 2500\AA is

d (Separation between two plates) = 65 cm

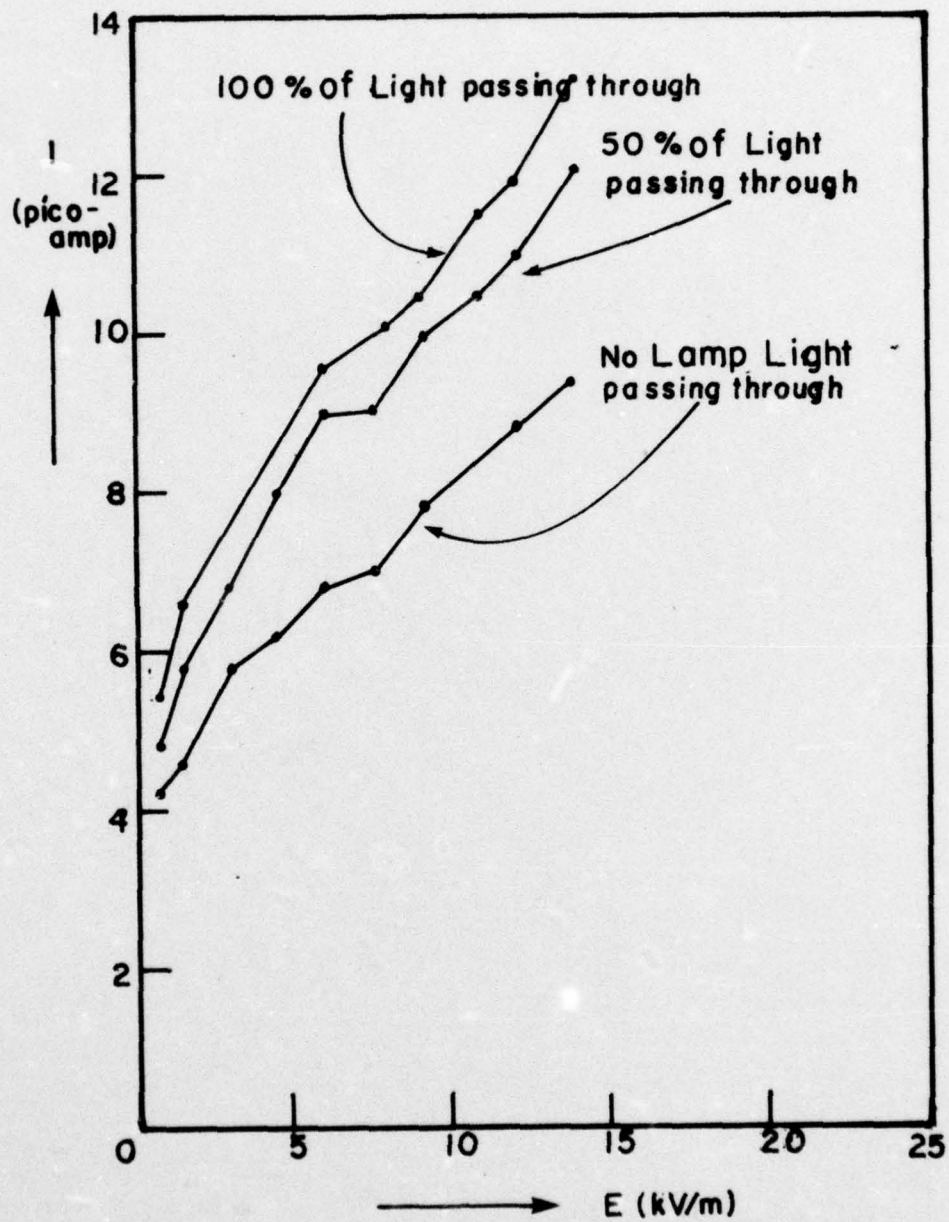
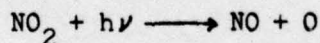


Figure 4.3

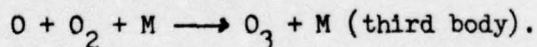
$$\begin{aligned}
 E &= h c / \lambda \\
 &= \frac{6.626 \times 10^{-27} \text{ erg-sec} \times 3 \times 10^{10} \text{ cm/sec}}{2500 \times 10^{-8} \text{ cm}} \\
 &= 8 \times 10^{-12} \text{ erg} \\
 &\doteq 5 \text{ eV}
 \end{aligned}$$

which is smaller than the ionization potential for ordinary air which is around 14 eV. This shows ordinary air molecules cannot be photo-ionized by 2500 Å UV light. One explanation of what the light does is to break up those intermediate and large ions in the air which are small ions with particulates attached to them. As a result, the small ion content increases and the air conduction current is increased as observed.

As another example, light in the range of 300-4600 Å can decompose nitric oxides in the air:



and



Ozone can then decompose oxygen and break up other particulates in the air from the energy released.

This is a possible explanation for the "sun-rise effect", the observed increase in the magnitude of the air-earth conduction current after sunrise.

At the same time, the work function (the energy needed to carry a charge across a metal vacuum boundary) for aluminum is about 4.2 eV and there might be extra ions from the aluminum plate surface into the air in this case.

(iii) Comparison between the measurements of current flowing through the hemisphere pair and that between the plates:

The hemisphere pair is suspended in the screenroom between the parallel plates. Current readings from the two systems in the presence of the applied electric field are taken simultaneously. A linear relationship is obtained in the Ohmic region (Figure 4.4). From the slope of the line and the given dimensions of the plates and the sphere, we can calculate the value of the factor K where

$$K = \frac{I_{\text{sphere}} / \pi r^2}{I_{\text{plate}} / A_{\text{plate}}}.$$

Theoretically, $K = 3$ for a sphere in a uniform field as derived in the previous chapter. But in this case, since the plates are of finite distance from the sphere, equipotential lines are distorted and are concentrated more toward the sphere than in the case of plates with infinite separation; the result shows $k > 3$. Furthermore, in the region of higher field intensity, the K value is higher than that in the region of the lower field strength, the sphere gets to the unsaturated region three times faster than for the parallel plates.

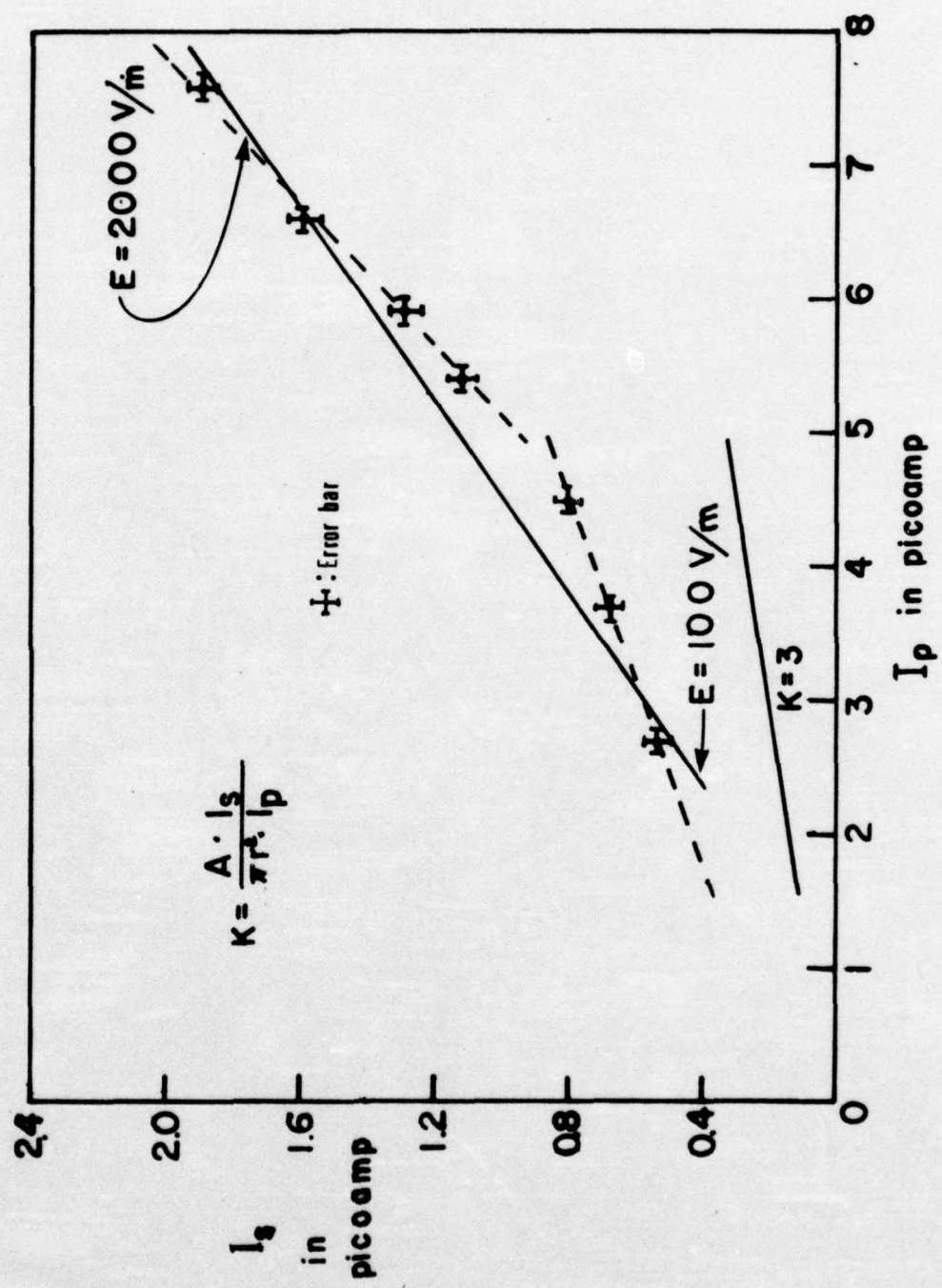


Figure 4.4

II. Outdoor Measurements

(1) Fair Weather Measurements

(1) Sunrise Effect

The "sunrise effect" of atmospheric electricity is the observed increase in the atmospheric electric field and current density after sunrise. It was first observed by Holzer (1955) and Kasemir (1956).

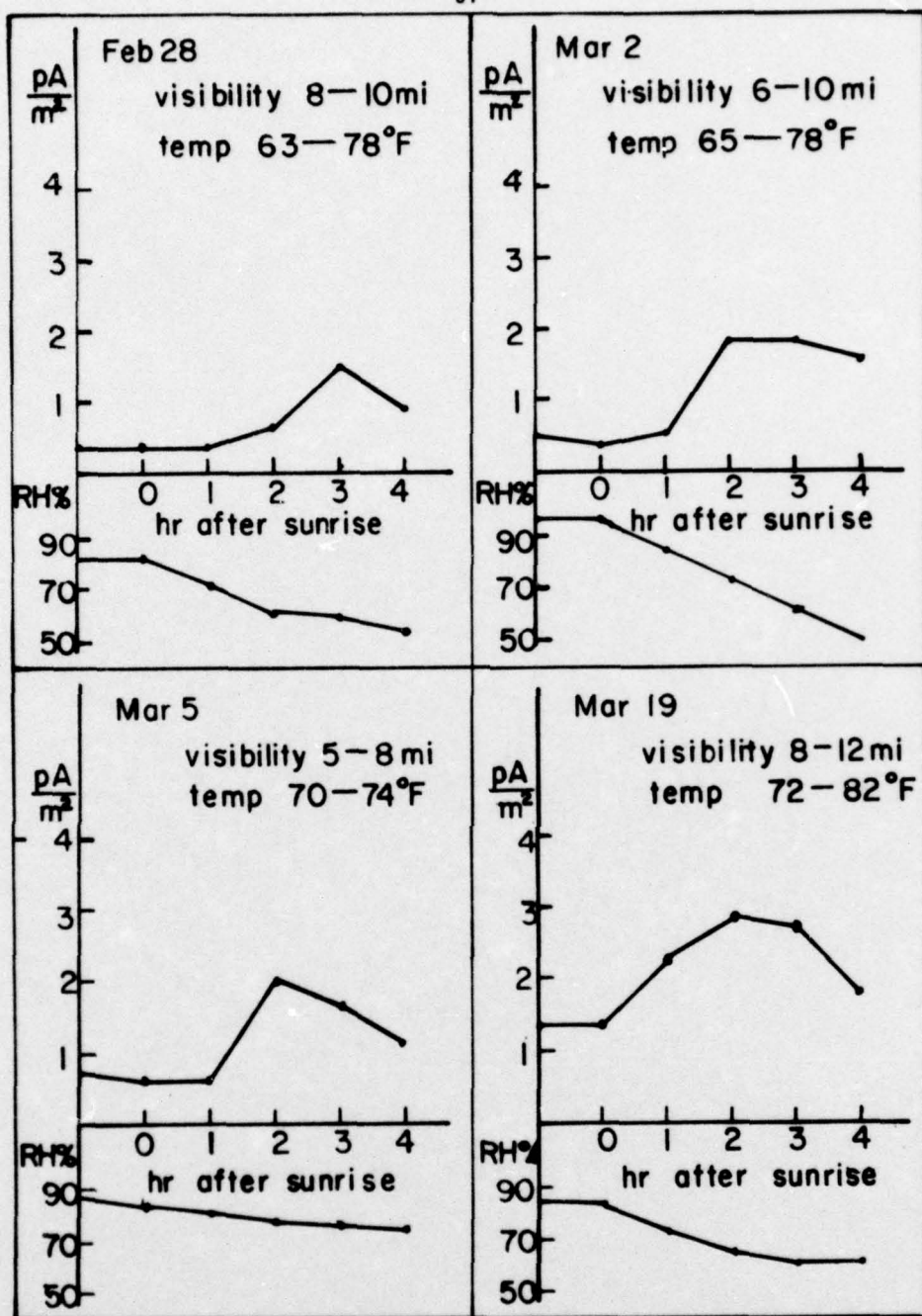
In this experiment, the sunrise effect has been extensively observed. On a clear, cloudless morning, a gradual increase in atmospheric conduction current reading is first observed about an hour after sunrise. The current density then gradually decreases but usually stops its decrease at a higher value than was observed before sunrise. At different times of the year, as the time of sunrise varies with local time, the current pattern shifts in the same manner.

On the other hand, on rainy, hazy or low cloud overcast mornings, we can not detect this effect. The sun does not have the large immediate effect on the near ground environment that is observed on the clear mornings. This is evidence that the sunrise effect is due directly to solar radiation and its warming effects.

Figure 4.5 shows some characteristic air conduction current variations after sunrise on clear days.

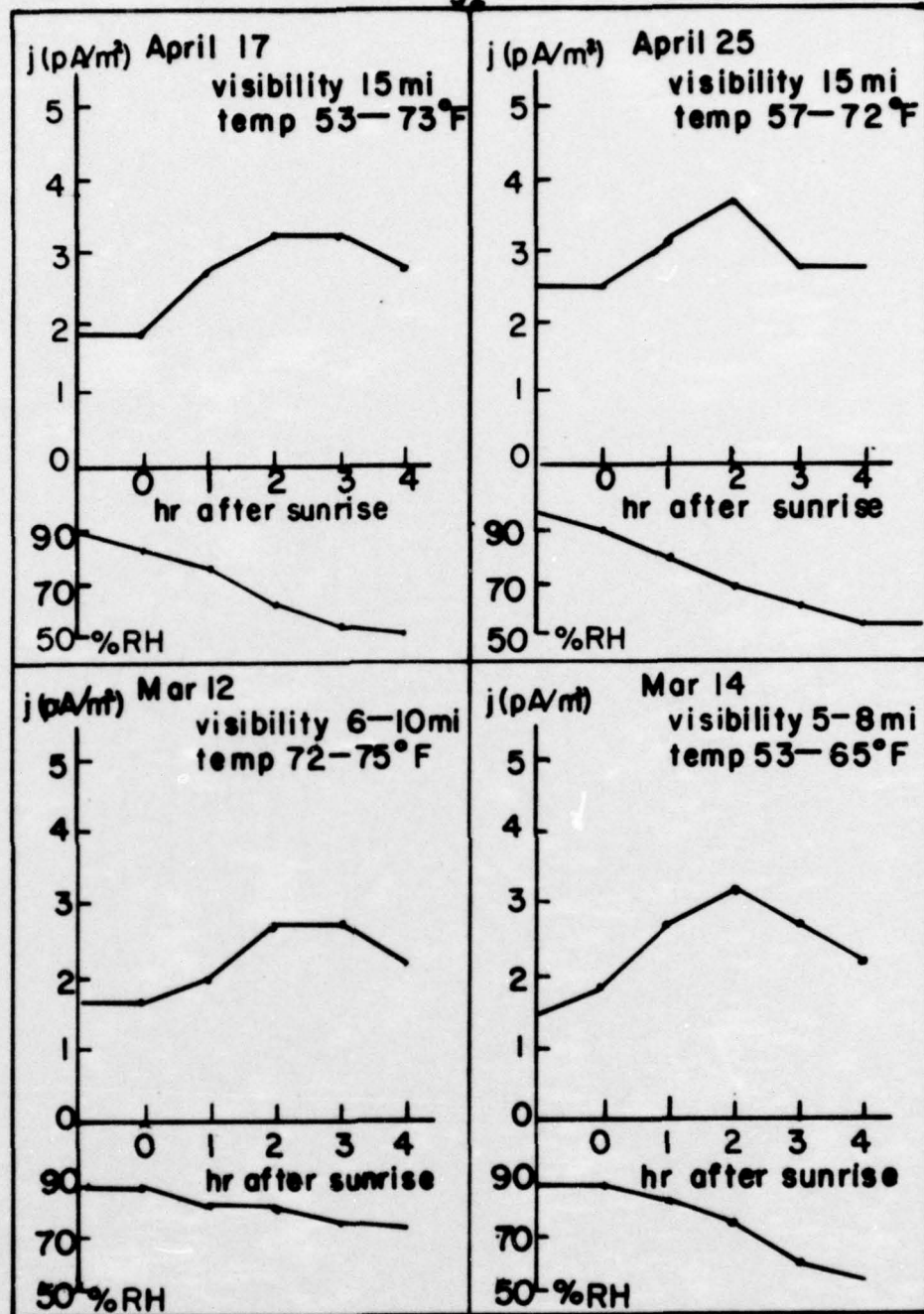
Mulheisen (1956) recorded the space charge density in addition to the electric field and the air-earth conduction current in and around Stuttgart, a medium-size industrial town in Germany. He found that most of the producers of man-made dust and smoke particles and condensation nuclei give them off as charged particles.

But this is proved not to be the cause of the sunrise effect.



the Sunrise Effect

Figure 4.5



the Sunrise Effect

Figure 4.5 (continued)

First of all, the pollutants are larger particulates. They have lower mobilities compared to small ions which are responsible for the air-earth conduction current. The correlation has been shown by Arnold (1974). Also, previous measurements at mountain stations where they are free of industrial influences do show the consistent existence of the sunrise effect under fair weather conditions.

There are several possibilities that are more reasonable for the cause of the sunrise effect:

1. The onset of convection when the earth's surface is heated up by the sun results in the mechanical transport of positive charge upward. This would cause the magnitude of the normal downward air-earth conduction current to increase at the same time. This hypothesis of the "Austausch generator" was first introduced by Kasemir in 1956.
2. Rapid increase of relative humidity after sunrise on a clear morning indicates the lower water vapor content due to evaporation. As a result, the mobility of ions is increased which increases the conduction current.
3. Solar radiation energy is absorbed directly by aerosols and large ions causing a separation of the small ions from the larger forms. This condition has been simulated in our laboratory as described in the previous section.

(2) Fog Effect:

Fog, one of the factors that usually obscures the sunrise effect, has been under observation by atmospheric scientists. The effects

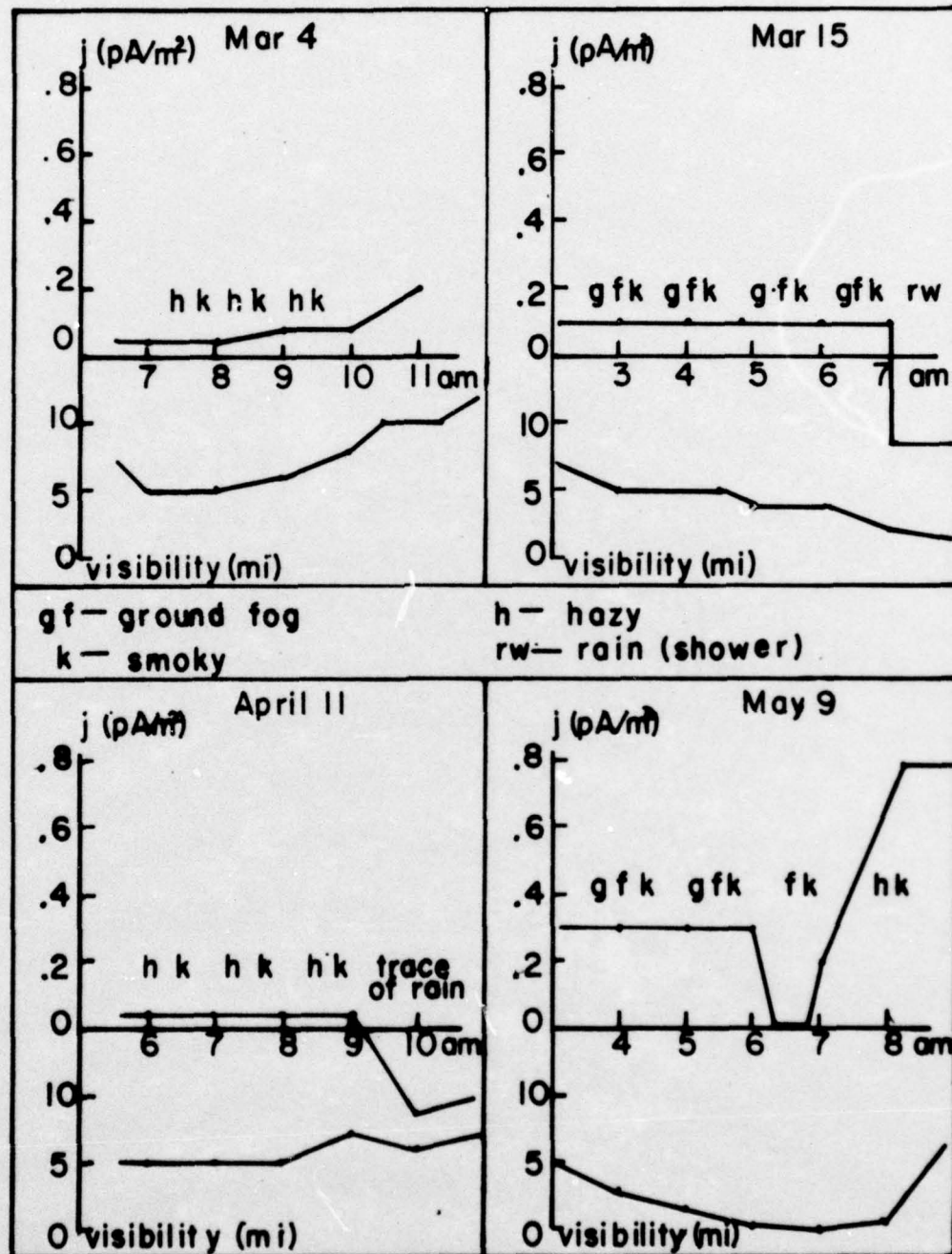
on atmospheric electric field, conductivity and conduction current during the growth, development and dissipation of fog have been studied.

According to our observations, conduction current decreases about one hour before the inception of fog, stays in a rather constant manner there, and increases again before the fog dissipation. The low reading is usually about 0.5 pA/m^2 , sometimes close to zero and occasionally when drizzle occurs, the current reading shows a small negative (opposite to normal) value. (See Figure 4.6).

These observations agree with Serbu and Trent (1958) and Dolezalek (1962). The atmospheric electric field and air conduction current measurements during wide spread fog showed a considerable increase in the electric field and a decrease in conduction current one to two hours before the onset of the fog and reverse changes appear $\frac{1}{2}$ to $1\frac{1}{2}$ hours before the dissipation of the fog.

An explanation for the phenomena is that the growing droplets, before the fog forms, capture the natural ions; this will decrease the mobility of ions and the conductivity of the air considerably which leads to a decrease in the air-earth conduction current and the atmospheric electric field is forced to increase to some extent. When the droplets begin to evaporate through absorbing infrared radiation from the sun and warming up from below from the earth, the thickness of the fog layer decreases and as a result, the columnar resistance of the air decreases. This increases the conduction current before the complete dissipation of the fog.

Thorough investigations both qualitatively and quantitatively of



Fog Effect

Figure 4-6

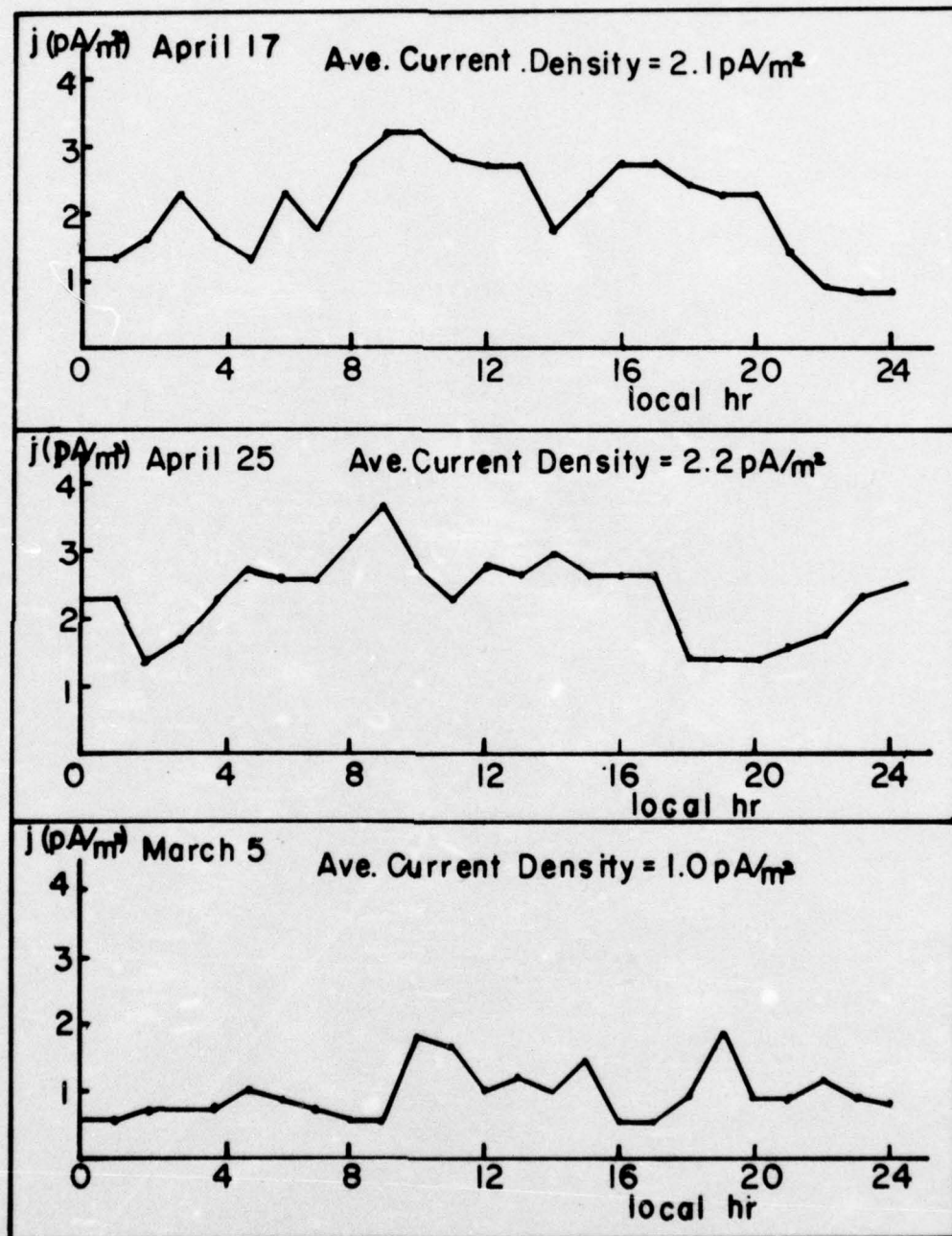
the electrical properties of fog will lead to a better understanding of the nature of fog and help in weather forecasting for safer aviation and sailing.

(3) Diurnal Variation

The daily pattern of air-earth conduction current (Figure 4.7) shows that at night, the current is relatively low and quiet. It rises in the morning and reaches the peak approximately two hours after sunrise (Ref. Section(1) Sunrise Effect) and then usually drops in its magnitude a little bit until later in the afternoon or early in the evening it reaches another relative maximum, probably due to less water content in the air from the heating of the earth. The current then drops its value and stays rather stable all night until the next day.

This pattern agrees with recent observations of Sharpless (1971). Furthermore, Israel (1973) summarized and compared many past works and showed that the diurnal variation of air-earth current density is not quite uniform over different places. But in general, most of them do have the similar pattern as ours.

There has been a lot of effort trying to correlate the data with atmospheric electric field intensity E and air-earth current density j but without too much success. Except above the oceans where E and j possess similar trends, atmospheric electric field generally follows a universal time variation — a minimum around 0400 hr and maximum around 1600-1800 hr Greenwich Mean Time, and on the other hand, air-earth conduction current varies mostly with local time and weather



Diurnal Current Variations
Figure 4.7

conditions as described. This shows that among the electrical parameters of the atmosphere, air conduction current is more dominated by local effects.

(4) Seasonal Trend

Since we only have several months' accumulation of air-earth conduction current data, conclusion on the seasonal variation can not be drawn. But there is one trend we observed. During the winter months the current density average is generally lower than that in the summer. (See Figure 4.7 for comparison.) In February, for example, the typical daily average is about 1.0 pA/m^2 and in May it jumps up to 2.2 pA/m^2 . This can be explained by the fact that the frequency of lightning activity is higher in the summer than in the winter, negative charge is brought down to the earth in greater quantity which results in a higher fair weather conduction current in summer time.

*** The current we measured is only half of the true air-earth conduction current. However, we also have an extra field enhancement since the sphere was set up above the roof of the three-story building which should compensate for the current reduction to some degree.

(ii) Disturbed Weather Measurements

(1) Effects of low rain clouds and thunderclouds:

It has been accepted that a thundercloud consists of two portions of approximately equal and opposite charges of electricity, the upper part being mostly positively charged and the lower part negatively charged. The charge separation mechanism is not well understood yet. This dipolar construction will change the electric field intensity at an observer on the earth. The sign and magnitude of the change depend on the position of the cloud (Chalmers, 1958). Consider a cloud with dipolar construction with a charge of $+Q$ at height H_1 and a charge of $-Q$ at height H_2 , and the observer at a horizontal distance D from the cloud (Figure 4.8).

The change of vertical electric field strength due to the existence of the cloud is

$$\frac{2 Q H_1}{4 \pi \epsilon_0 (H_1^2 + D^2)^{3/2}} + \frac{-2 Q H_2}{4 \pi \epsilon_0 (H_2^2 + D^2)^{3/2}} \quad \begin{matrix} \text{(downward} \\ \text{positive)} \end{matrix}$$

This change is zero when

$$\frac{H_1}{(H_1^2 + D^2)^{3/2}} - \frac{H_2}{(H_2^2 + D^2)^{3/2}} = 0$$

or

$$D^2 = H_2^2 H_1^2 (H_1^2 + H_2^2)$$

$$D = H_1^{1/3} H_2^{1/3} (H_1^2 + H_2^2)^{1/2}$$

In other words, when $D < H_1^{1/3} H_2^{1/3} (H_1^2 + H_2^2)^{1/2}$ the cloud of positive polarity produces a negative effect on the electric field strength at the observer's position, beyond that limit the effect is positive.

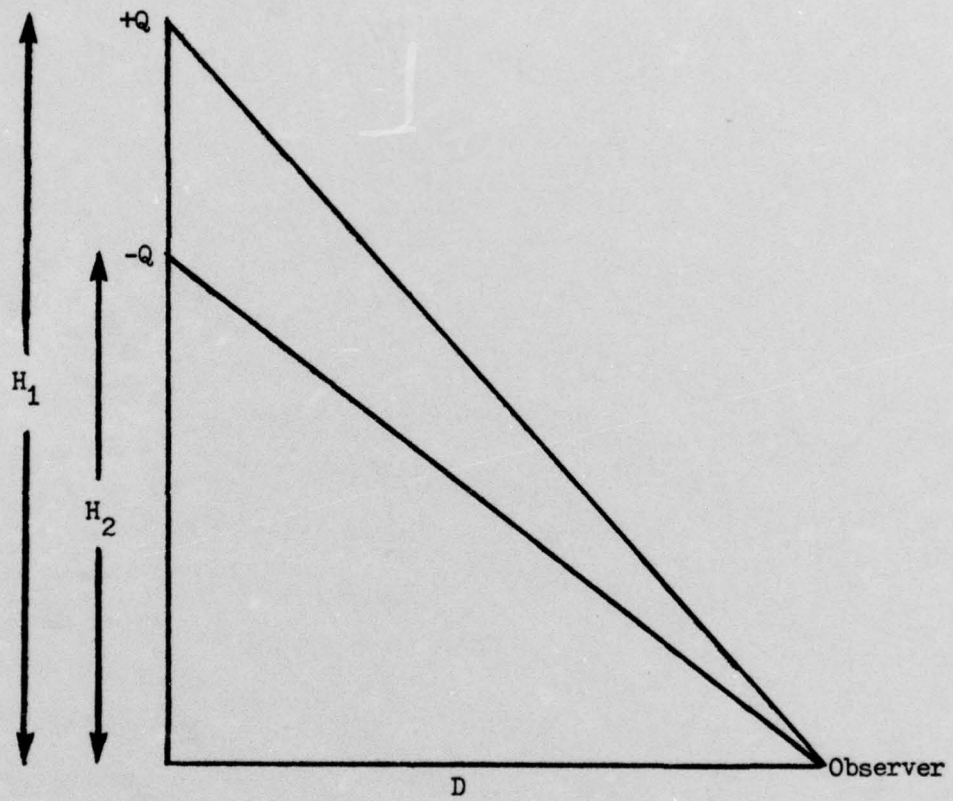


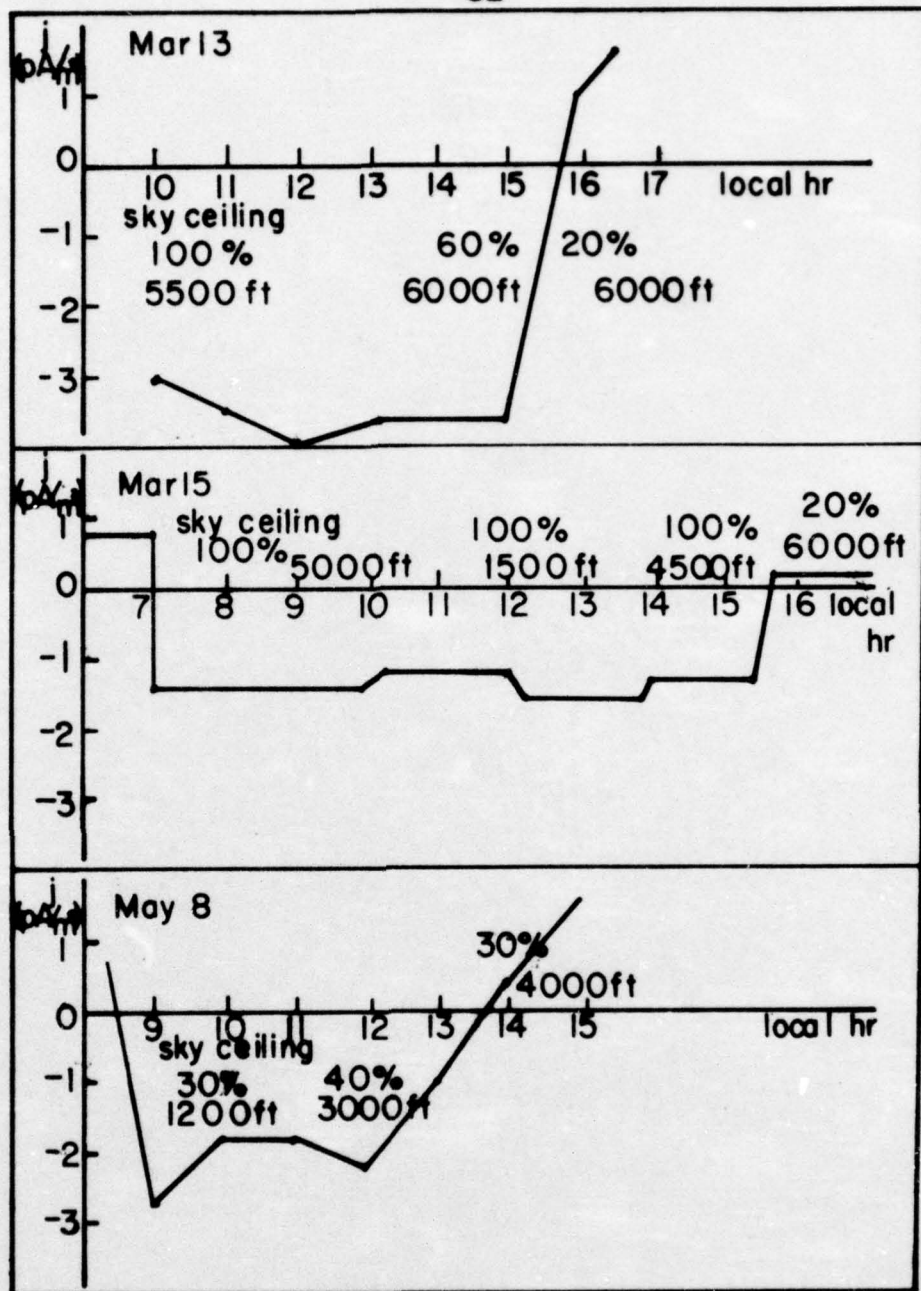
Figure 4.8

As for the special case of overhead or overcast clouds, the effect is always negative independent of the height of the cloud. In other words, it will decrease the normal downward atmospheric electric field intensity, and, if the clouds get close (low in altitude) enough, it will change the direction of the field.

From the fact that negative current readings are usually observed during times of overcast low clouds (Figure 4.9) we can reach the conclusion that most of the low cumulus, cumulonimbus and stratus clouds do have the same charge separation property. Some of these clouds would produce both lightning flashes and precipitation, others would not. But the effects are the same.

To demonstrate the situation, we consider clouds of thickness H completely overcast, the height of the cloud base being h_1 . To simplify the situation, we consider a cylindrical portion of the sky with its base coincide with the cloud base. Assume the base diameter to be $2a$, large compared to either h_1 or H , which in this case is the height of cylinder. If charge separation does exist in clouds, we can calculate the electric field intensity experienced by the observer on the ground produced by the dipolar construction of the clouds with different charge concentrations.

Suppose the cylinder is composed of three parts (Figure 4.10a), the lower part with charge concentration density $-\rho$ distributed from heights h_1 to h_2 , the middle part being well mixed of charges of both signs and the upper part with charge density $+\rho$ from h_3 to h_4 . We start from a disk of thickness dh with surface charge density σ



the Effect of Low Clouds

Figure 4.9

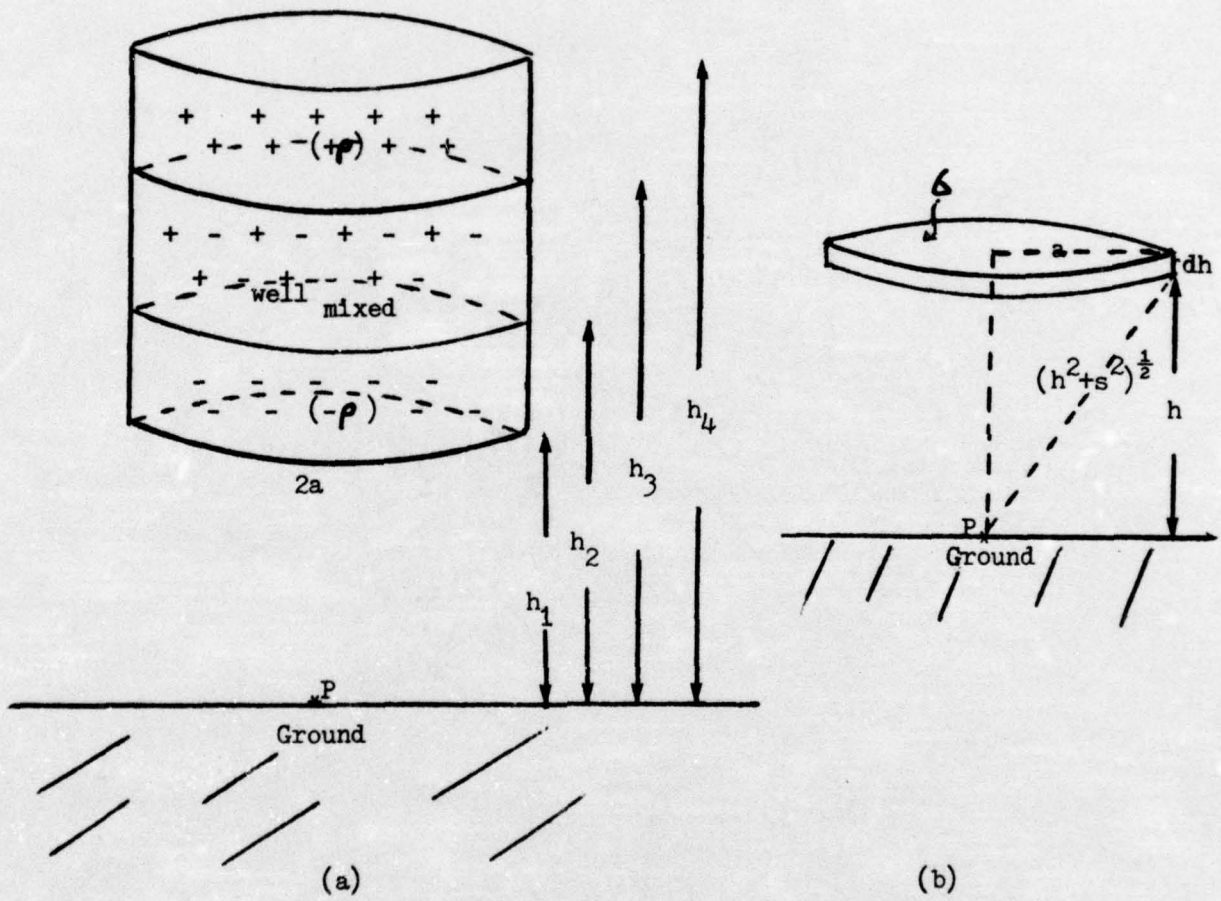


Figure 4.10

at height h (Figure 4.10b).

The field at P is

$$\begin{aligned}
 E(0, h, 0) &= 2 \frac{1}{4 \pi \epsilon_0} \int \frac{dq}{r^2} \\
 &\quad \text{(Factor 2 comes from the image charge)} \\
 &= \frac{2}{4 \pi \epsilon_0} \int_{s=0}^{s=a} \frac{2 \pi \sigma s}{h^2 + s^2} ds \\
 &= \frac{\sigma}{\epsilon_0} \int_0^a \frac{s}{h^2 + s^2} ds \\
 &= \frac{\sigma}{2 \epsilon_0} \ln(h^2 + s^2) \Big|_0^a \\
 &= \frac{\sigma}{2 \epsilon_0} \left[\ln(h^2 + s^2) - 2 \ln h \right]
 \end{aligned}$$

Then we consider a uniformly charged cylinder of charge density from height h_1 to h_2 :

$$\begin{aligned}
 \rho &= \frac{dq}{dA dh} & \rho dh &= \sigma \\
 dE &= \frac{\rho}{2 \epsilon_0} dh \left[\ln(h^2 + a^2) - 2 \ln h \right].
 \end{aligned}$$

Field E at P due to the cylinder ($h_1 \rightarrow h_2$) is

$$\begin{aligned}
 E &= \frac{\rho}{\epsilon_0} \int_{h_1}^{h_2} \left[\frac{1}{2} \ln(h^2 + a^2) - \ln h \right] dh \\
 &= \frac{\rho}{\epsilon_0} \left[\frac{h}{2} \ln(h^2 + a^2) - h + a \tan^{-1}\left(\frac{h}{a}\right) - h \ln h + h \right]_{h_1}^{h_2} \\
 &= \frac{\rho}{\epsilon_0} \left[\frac{h}{2} \ln(h^2 + a^2) + a \tan^{-1}\left(\frac{h}{a}\right) - h \ln h \right]_{h_1}^{h_2}.
 \end{aligned}$$

So the electric field change at P on the ground due to the cloud cylinder would be:

$$\begin{aligned}
 E_{\text{change}} &= \frac{\rho}{\epsilon_0} \left\{ \left[\frac{h}{2} \ln(h^2 + a^2) + a \tan^{-1}\left(\frac{h}{a}\right) - h \ln h \right]_{h_1}^{h_2} \right. \\
 &\quad \left. - \left[\frac{h}{2} \ln(h^2 + a^2) + a \tan^{-1}\left(\frac{h}{a}\right) - h \ln h \right]_{h_3}^{h_4} \right\}.
 \end{aligned}$$

This is an upward field which is opposite to the normal direction of the atmospheric electric field. We can compare this value with the normal atmospheric electric field intensity which is about 130 volts/m. If the change exceeds this value, the field direction on the ground is reversed.

The altitude of typical overcast clouds that gives us negative current readings near ground is about 1 km (~ 3000 ft) or even less. The vertical thickness is about 3 km. We can estimate the charge distribution required to reverse the atmospheric electric field from the above derived equations. Assume the following:

Cell base altitude: 1 km.

Negatively charged region: 1 km \rightarrow 2 km.

Mixed region: 2 km \rightarrow 3 km.

Positively charged region: 3 km \rightarrow 4 km.

Or equivalently:

$$\begin{aligned} h_1 &= 1000 \text{ m,} \\ h_2 &= 2000 \text{ m,} \\ h_3 &= 3000 \text{ m,} \\ h_4 &= 4000 \text{ m.} \end{aligned}$$

And consider the cylindrical region with $2a = 10,000 \text{ m}$ or $a = 5000 \text{ m}$.

The result is as follows:

ρ (coul/m ³)	E (V/m) upward	E (V/m) downward	E _{net} (V/m) change upward	Remarks
3×10^{-13}	43.1	19.0	24	< 130 V/m
10^{-12}	143.2	63.2	80	< 130 V/m
3×10^{-12}	429.6	189.6	240	> 130 V/m
10^{-11}	1432.0	632.0	800	> 130 V/m

We see for the cloud thickness considered, the atmospheric field direction will be reversed at about $\pm 3 \times 10^{-12}$ coul/m³ of charge concentration for the dipolar construction of the cloud. This is typical for space charge concentration inside a rain cloud (e.g. Takahashi, 1973) (3×10^{-12} coul/m³ $\doteq 10^{-8}$ esu/cm³). Actually it is not a high charge concentration. The total charge involved is only one Coulomb in the upper part and negative one Coulomb in the lower part inside the 10 km diameter cylindrical region which can either be a single cell or a linear combination of several cells.

Inside a thundercloud, the degree of separated charge concentration is much higher. Typical values are ± 10 to ± 30 C. We can show through calculations that thunderclouds can change the normal atmospheric field direction on the ground at much higher altitudes than ordinary or precipitation clouds which possess lower charge concentrations.

Assume the cell cylinder of the same dimensions, but of different altitudes with different charge concentrations, we get the following result (where $\pm 3 \times 10^{-11}$ coul/m³ corresponds to ± 10 C of total charge in the charge separated regions):

Base Altitude (m)	(coul/m ³)	E _{upward} (volts/m)	E _{downward} (volts/m)	E _{net change} (volts/m)	Remarks
2000	+10 ⁻¹² from 4000 to 5000 m well mixed in between	45.7	91.8	46.1	< 130 V/m
2000	+10 ⁻¹¹ " well mixed in between	457	918	461	> 130 V/m
2000	+3x10 ⁻¹¹ " well mixed in between	1370	2573	1383	> 130 V/m
3000	+10 ⁻¹² from 5000 to 6000 m well mixed in between	63.3	34.2	29.1	< 130 V/m
3000	+10 ⁻¹¹ " well mixed in between	632.6	341.8	290.8	> 130 V/m
3000	+3x10 ⁻¹¹ " well mixed in between	1898	1025	872	> 130 V/m

Another question now arises: If low rain clouds and thunder clouds reverse the direction of the normal atmospheric electric field below them, what about the situation above these clouds? Based on the electrical structure of the cloud, the electric field above the clouds should also be opposite to fair weather field direction if the theory of charge separation inside a cloud holds. This has actually been observed through balloon and aircraft probes (e.g. Weed and Kellogg, 1974).

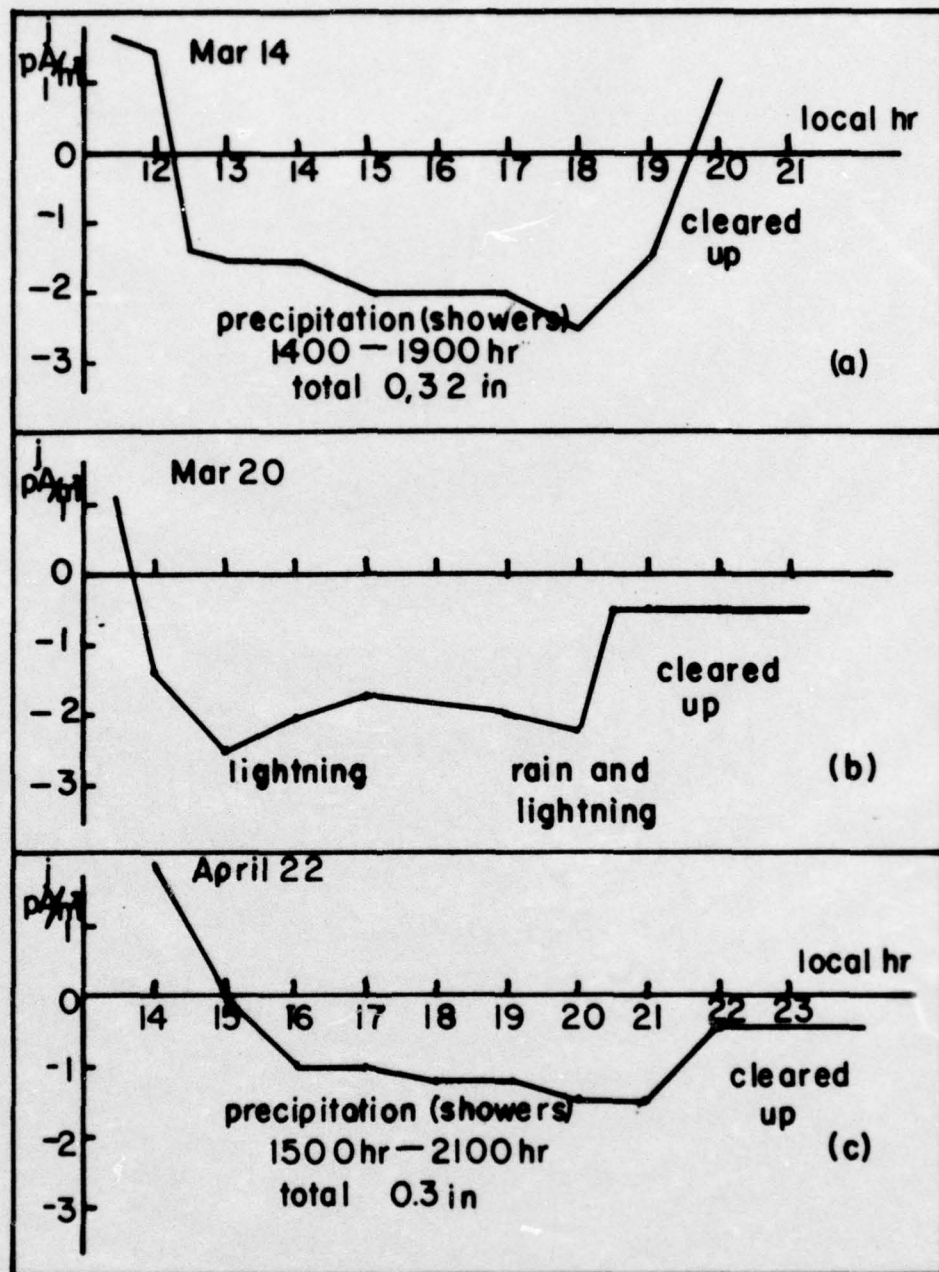
(2) Current during Precipitation

In Takahashi's review paper (1973), it was concluded that for rain clouds, negatively charged droplets predominated at the lower part of the cloud, and positively charged cloud droplets at the upper part. This agrees with our observation of negative air conduction current at ground under low overcast clouds even before the rain.

During times of showers or continuous rain, negative current readings with absolute magnitude usually smaller, not exceeding 2.5 pA/m^2 , (See Figure 4.11) are observed.

Raindrops are observed to be charged carriers. The amount of charge per drop varies with its size and also with the downfall speed. Measurements of other investigations (Takahashi, 1973) show they vary from $-3 \times 10^{-15} \text{ C}$ to $+10^{-10} \text{ C}$ per drop.

It is difficult to draw a conclusion of droplet charge in terms size of the drop, the position of the drop inside the cloud and the type of the cloud. Different in-cloud observations have



Effect on Current during Precipitation

Figure 4.11

different conclusions. It is therefore logical to assume drops leaving the cloud without any sign predominance.

Precipitation current of negative value but smaller in magnitude can then be explained as follows:

The vertical electric field is set up first. As described in Section (ii) (1), it is a negative (opposite to normal) field with respect to ground which results in a negative conduction current. The induced charge on the earth will be positive so that the droplet, regardless of its original net charge, will get induced negative charge at the lower part and induced positive charge at the upper part. Because of this surface charge distribution and with the atmospheric ions flowing around the falling droplet, a droplet can acquire a positive charge by capture of positive ions on the negatively charged bottom as it falls down in the air (Wilson's Theory, 1929). This explains why most people observe more positively charged raindrops at ground.

This effect gives a positive (downward) current as droplets capture positive ions from the air. But the magnitude of this positive current can not exceed that of the total negative air conduction current resulted from the negative field. This results in the observed negative precipitation current of smaller magnitude. In the case of heavy rainfall this effect can compensate all the negative conduction current. Under this situation, the continuous near-zero current reading is observed.

At the same time, we also face the fact that even if precautions were taken for the rain, the insulating disk may lose its effect during heavy rainfall which will also result in a near-zero current reading.

(3) Post rain- or thunder-storm current

In the previous paragraphs we showed that during rain- or thunder-storms, the air-earth conduction current is negative. According to our current data, after a rain- or thunder-storm, in other words, after some amount of water has fallen on the ground, the current reading remains negative for quite a while even after the sky is all cleared up. This lasts from a couple of hours to as long as half a day (Figure 4.11 b,c) which is quite different from the cases after short showers, traces of rain or low clouds.

One possibility is that lightning flashes bring large amounts of negative charge to earth and its surrounding air so that with the excess negative charge in the air, the conduction current is bound to remain negative till the air is neutralized. Then the positive air conduction current will again flow in the positive atmospheric electric field.

But this is not likely the source for the excess negative charge in the air. All the negative charge brought down by lightning flashes will go into the ground right away instead of leaking to the air. Furthermore below the clouds the ground is positively charged as are the lightning channels; thus, the charge in the air could be of either sign.

From the previous section, it was showed that falling droplets acquire positive ions in the air. As a result, there will be a net negative charge left in the air. This negative space charge can be one source for the negative current after rain.

The theory related to waterfall electricity can also explain

our problem of negative current reading after rainstorms. Negative space charge near a waterfall was first discovered by Tralles in 1786. Lenard (1892) proved its existence and supported the theory that waterfall electricity was generated by electrostatic induction. Pierce and Whitson (1965) showed the existence of negative electric field near a waterfall due to negative space charge. Recent measurements give the result of space charge density of the order of 10^{-8} coul/m³ which extends to several kilometers from the falls (Boek, 1973).

According to Lenard, the presence of an electrical double layer at the surface is responsible for the electrification produced when water disrupts. The surface layer of water contains an excess of OH⁻ ions, and the H⁺ ions tend to reside in the bulk of liquid. Thus a removal of the surface layer by mechanical disintegration introduces negative charge into the atmosphere.

The same condition should also exist when there is a large amount of rain falling on the ground causing the splashing of water. The extra negative space charge will then reside in the neighbor air for some time. This should suffice to explain for the observed negative conduction current after a rain storm.

To estimate the time of neutralization, we can use the same equation derived for charged clouds, $E = \frac{\rho}{\epsilon_0} \left[\frac{h}{2} \ln(h^2+a^2) + a \tan^{-1}h/a - h \ln h \right]_{h_1}^{h_2}$. Assume a column extended right above the earth with $h = 100\text{m}$ and $a = 200\text{m}$. For $\rho = -10^{-11}$ coul/m³, we get $E = -1400$ volts/m (upward). If $j = -2 \times 10^{-12}$ A/m² (upward), the time of neutralization is about 2 hours.

III. Conclusion and Modification of the Theory of Charge Balance

In the previous sections, we discussed the general variations on air-earth conduction current density, the fair weather pattern and also observations during disturbed weather. The direction and magnitude of current under different conditions were discussed and explanations offered for their behavior.

As discussed in Chapter 1, it has been accepted that the most probable mechanism which keeps the balance of the charge of the earth through fair weather air-earth conduction current is lightning activity. Through this experiment, we realize that lightning activity is not the only mechanism that brings the negative charge to the earth. As proved in the previous section, low clouds which reverse the normal atmospheric electric field do bring negative charge to the earth. Of course the amount of charge they carry is less than lightning flashes (each cloud to ground lightning stroke can bring down several coulombs of negative charge). Nonetheless for regions and seasons of less lightning activity, clouds (and perhaps snow flakes too, which we didn't have a chance to test during the performance of the experiment) must contribute a portion for the mechanism of bringing negative charge to the earth. Only careful observation can determine the magnitudes of the various components.

IV. Future Prospects

Atmospheric electricity, though first discovered more than a hundred years ago, is a new branch of physical sciences of less than forty years of development. It can be divided into two categories: the fair weather electricity and the disturbed-weather electricity. It is also accepted that the disturbed-weather electricity acts like the "generator" of the atmospheric electricity and the fair-weather electricity, on the other hand, is the "consumer".

Through this experiment, we realize the future development should involve the following:

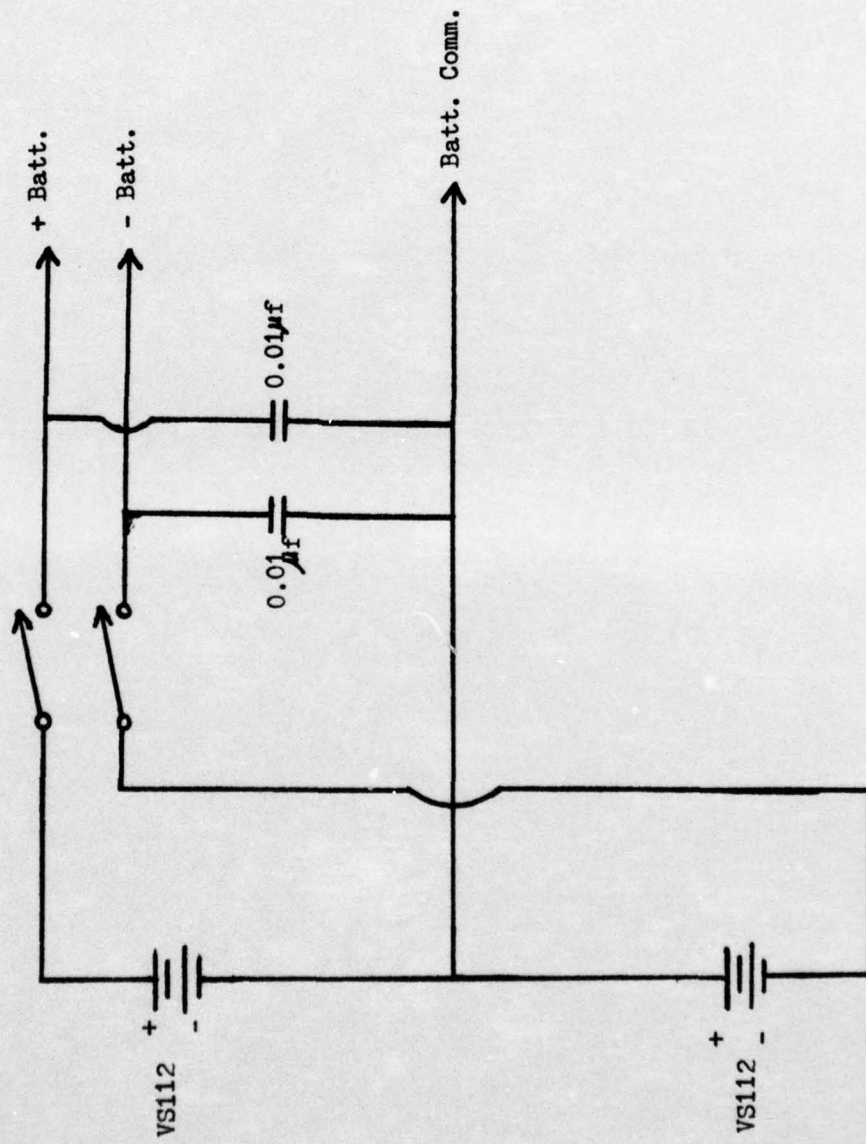
- (1) Long range measurements at different locations are needed in order to get a thorough picture of the global atmospheric electricity variation. This is due to the observed fact that local effects usually dominate the global influences on atmospheric electricity.
- (2) Measurements of the air-earth current density, together with the electric field intensity and the conductivity should be made simultaneously. In this experiment, it has been difficult to interpret different phenomena merely from the current density data. Only qualitative conclusions can be reached. With all the three parameters, we will be able to tell more about what is really going on, both qualitatively and quantitatively.

In short, atmospheric electricity is an exciting and challenging field to survey. Some of the applications include aids for practical meteorological work and detecting the effect of artificial radio-activity in the air. And above all, it can help us in developing a better understanding of our own atmosphere.

Appendix

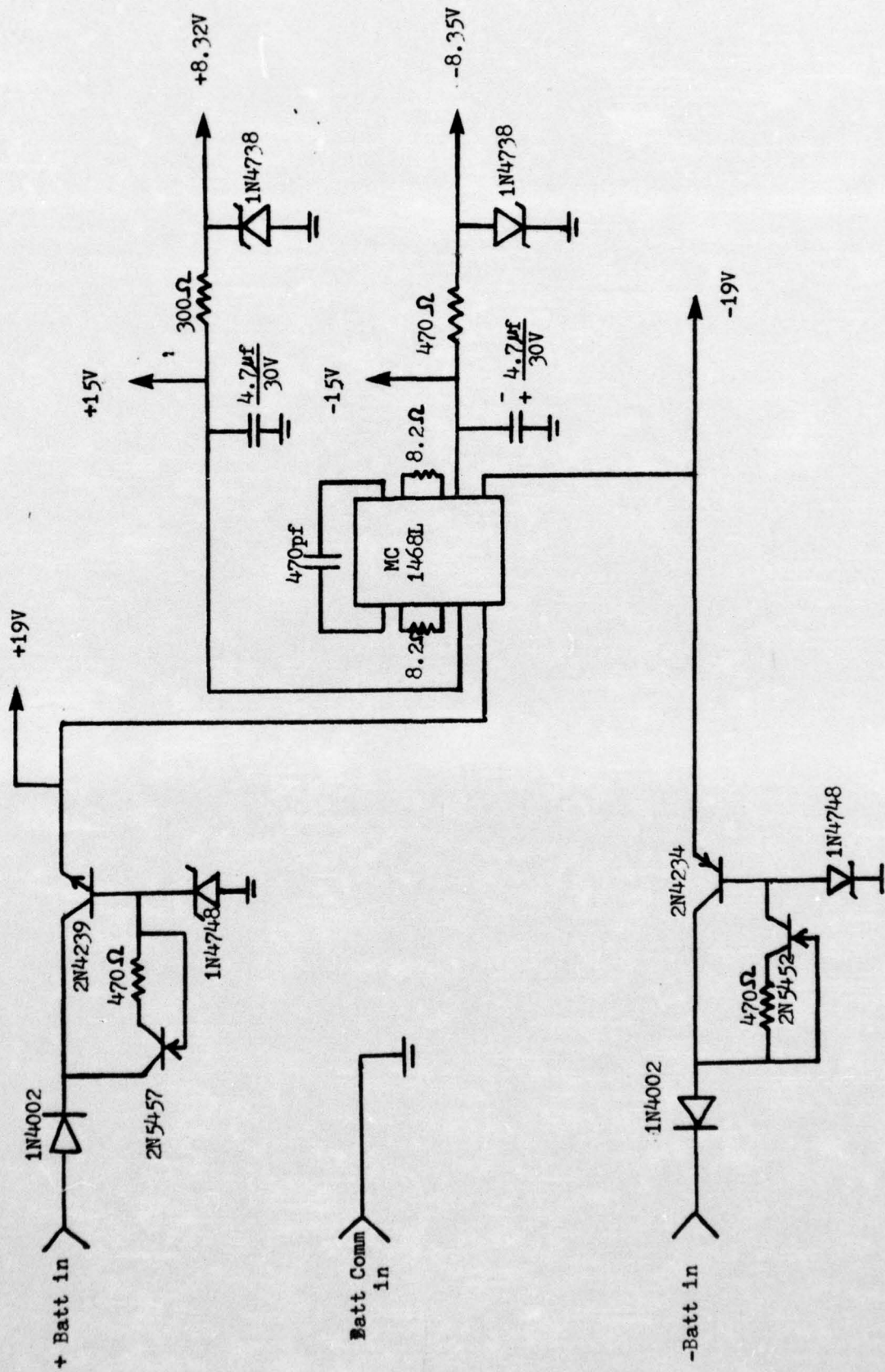
Circuit Diagrams

A1



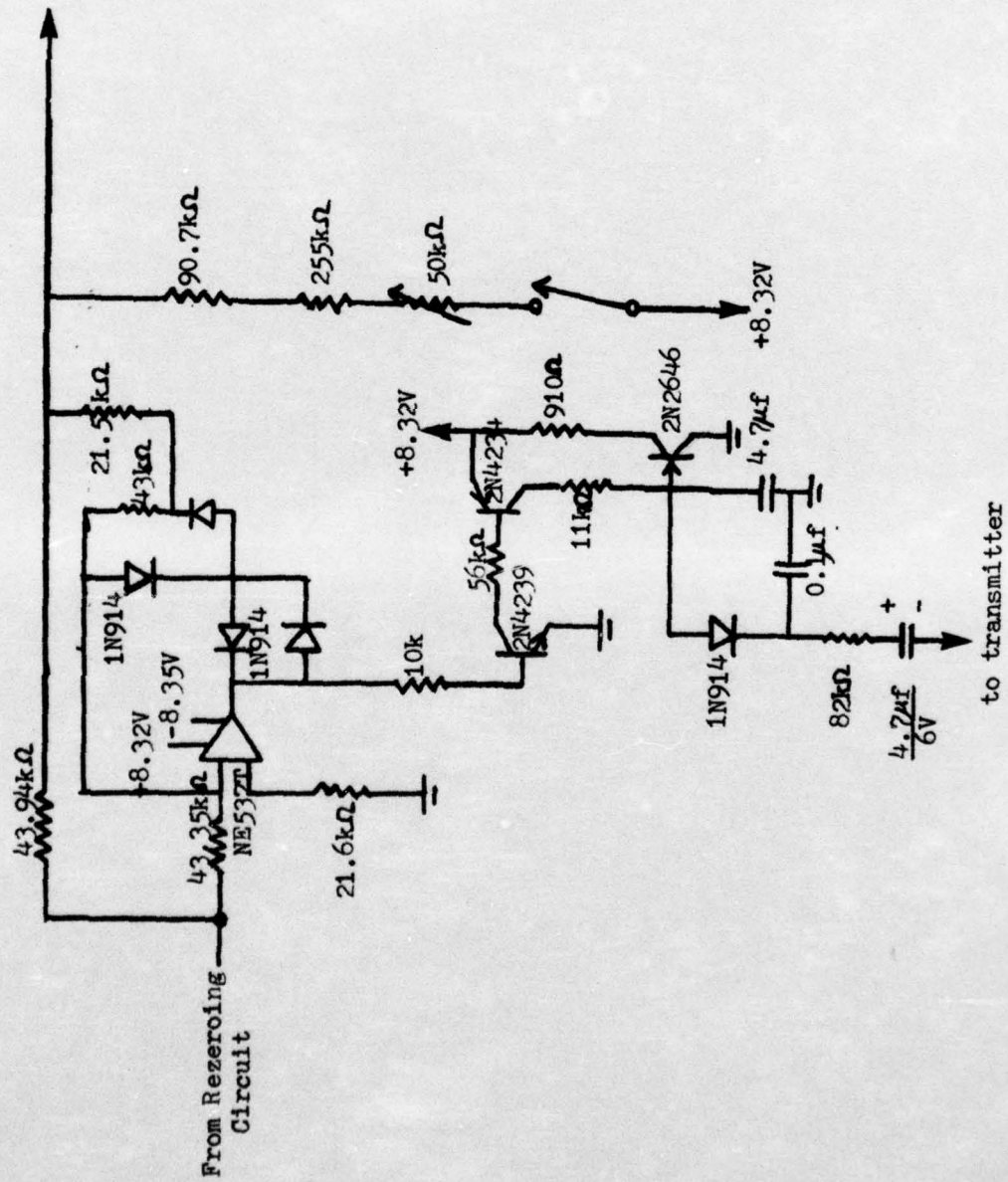
Battery Circuit

A2

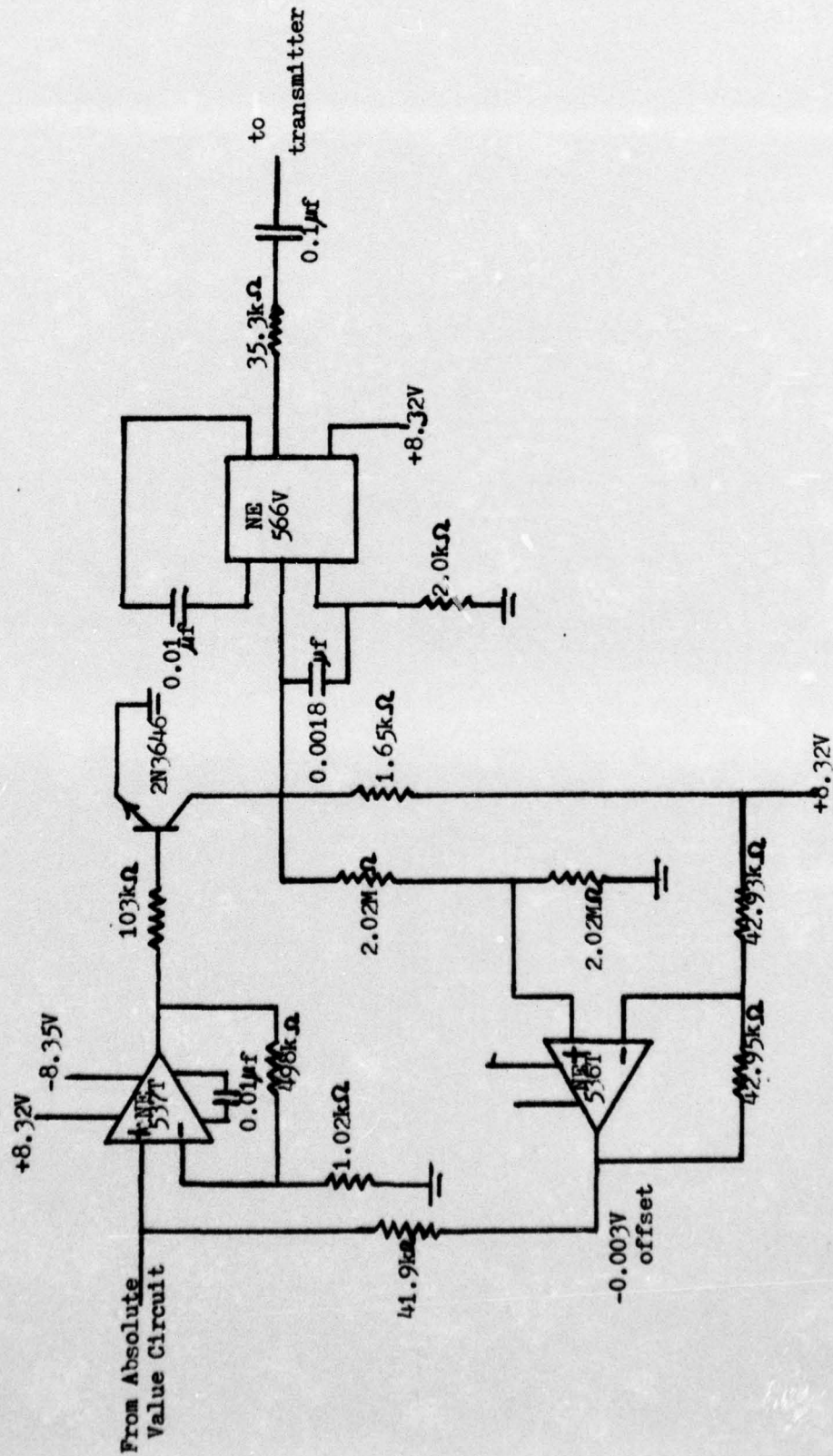


Voltage Regulator Circuit

To Level Shift to
V.C.O.

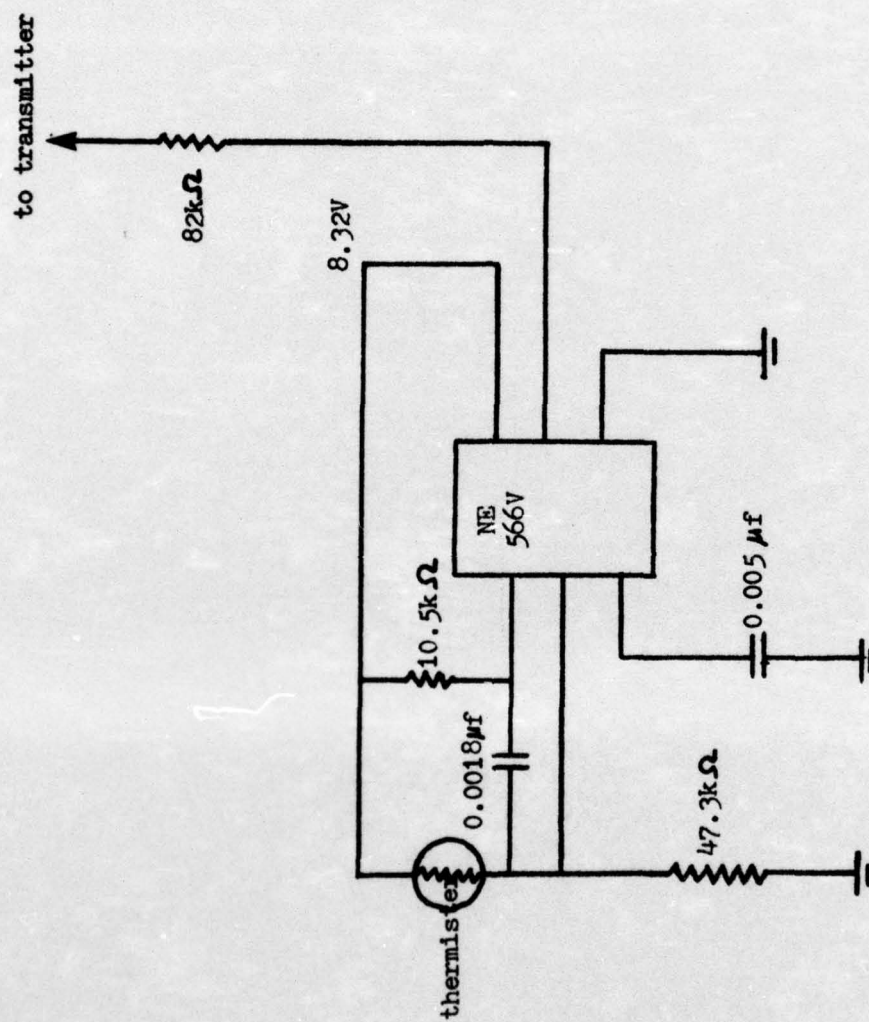


Absolute Value Circuit



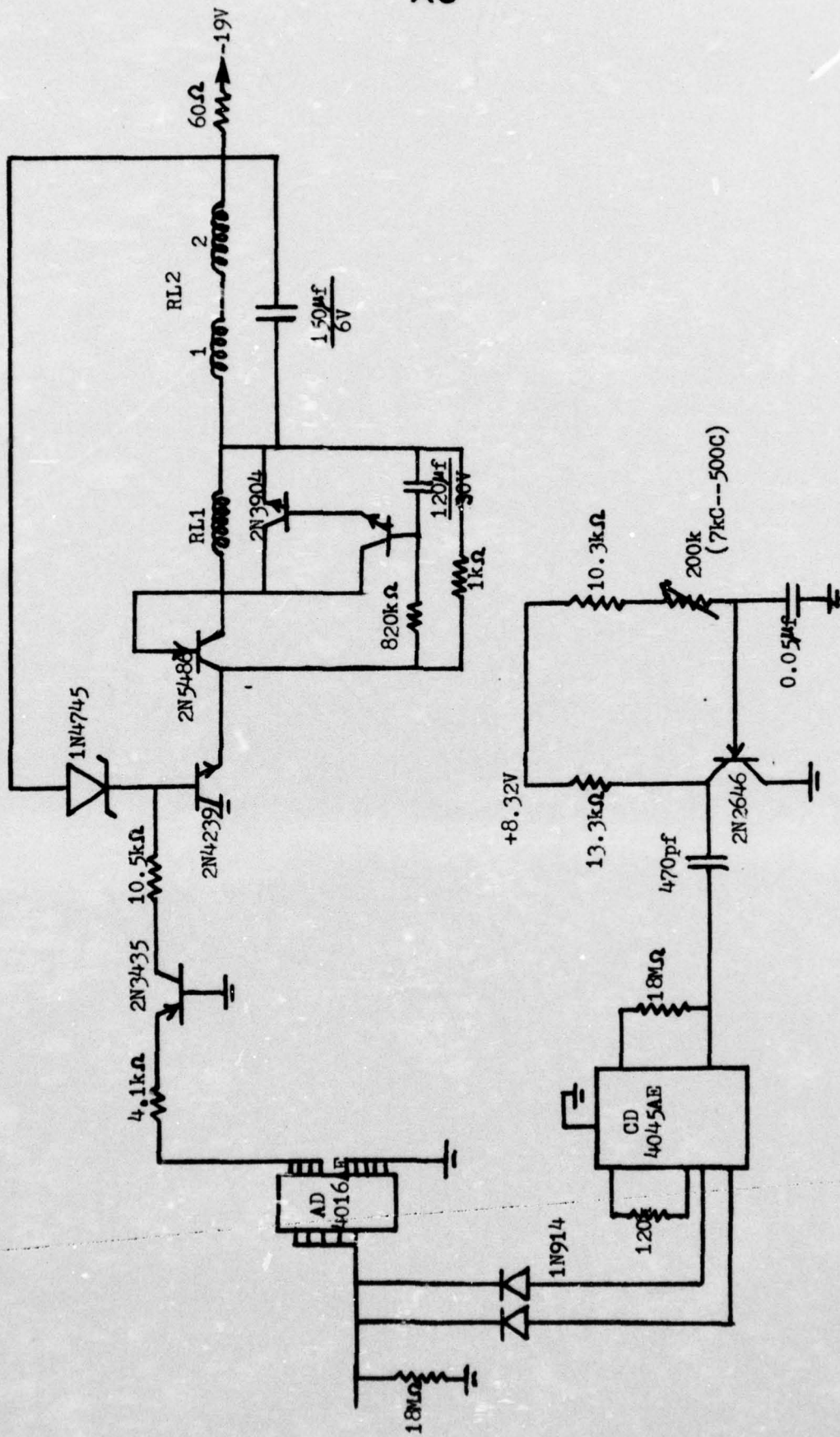
Circuit Diagram of Level Shift to Voltage Controlled Oscillator
and Voltage Controlled Oscillator

A5



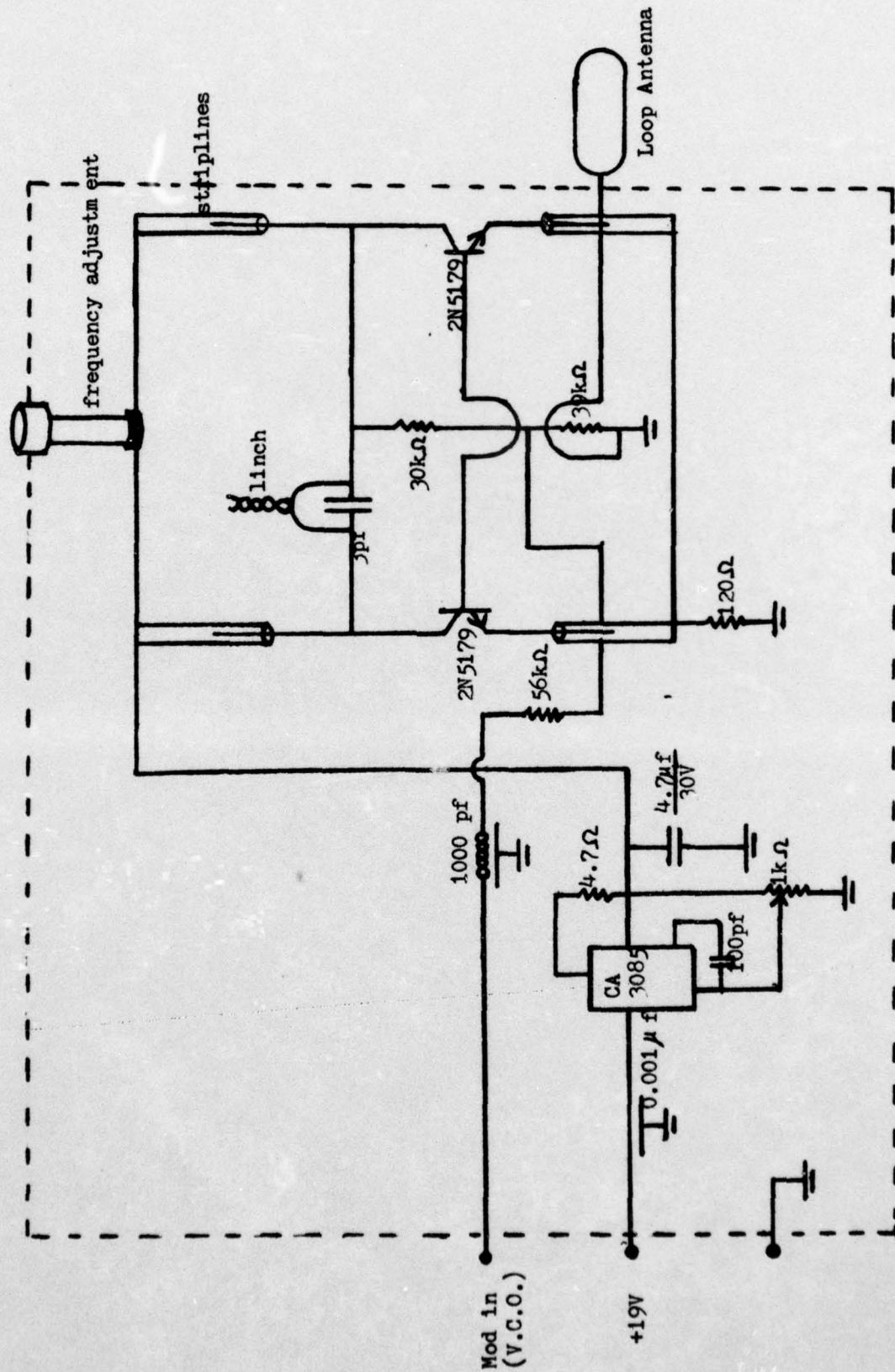
Thermister Circuit

A6



Master Clock Circuit

A7



408 Mc FM Oscillator

ACKNOWLEDGEMENTS

I am indebted to my thesis advisor, Professor Arthur A. Few, for the motivation of this investigation and the many valuable discussions of the thesis. Special thanks are due to Mr. Stephen Hurder for his ingenious design incorporated in the electronics; this instrumentation made the experiment possible. I am also grateful to Mr. Wayne Smith for his suggestions and help during the initial stage of the project.

This research and instrument development has been supported by: (1) the Atmospheric Program of the Office of Naval Research Contract Number N00014-67-A-0145-0004 and (2) the National Aeronautics and Space Administration's supporting Research and Technology Grant NGL44-006-012. A Patent Application has been filed on the instrument described in this thesis; Navy Case 56, 763.

REFERENCES

1. Adamson, J., The Compensation of the Effects of Potential Gradient Variation in the Measurement of the Atmospheric Air-Earth Current, Quart. J. R. Met. Soc., 86, 252-258, 1960.
2. Allen, C. W., Astrophysical Quantities (3rd Edition), Univ. of London, The Athlone Press, 1973.
3. Anderson, R. V. and E. M. Trent, Atmospheric Electricity Measurements at Five Locations in Eastern North America, J. of Applied Meteorology, 8, 707-711, 1969.
4. Arnold, J. A., The Use of Air Ion Mobility Spectrum Analysis to Determine Air Pollution, M. S. Thesis, Rice University, 1974.
5. Aspinall, W. P., Mechanical Transfer Currents of Atmospheric Electricity, J. of Geophysical Research, 77(18), 3196-3203, 1972.
6. Boek, W. L., Waterfall Electricity, Invited Paper, EOS, Trans. Amer. Geophys. Union, 54(11), 1102, 1973.
7. Chalmers, J. A. and E. R. W. Little, Currents of Atmospheric Electricity, Terr. Magn. Atmos. Elect., 52(2), 239-260, 1947.
8. Chalmers, J.A., The Electricity of Nimbo-Stratus Clouds, Pro. 2nd International Conference on Atmospheric and Space Electricity, 309-316, 1958.
9. Chalmers, J. A., The Measurement of the Vertical Electric Current in the Atmosphere, J. Atmosph. Terr. Phys., 24, 297-302, 1962.
10. Cobb, W., Oceanic Aerosol Levels Deduced from Measurements of the Electrical Conductivity of the Atmosphere, J. of Atm. Sciences, 30, 101-106, 1973.
11. Crozier, W. D., Electrode Effect during Nighttime Low-Wind Periods, J. Geophys. Res., 68(11), 3452-3458, 1963.
12. Crozier, W. D., Measuring Atmospheric Potential with Passive Antennas, J. Geophys. Res. 68(18), 5173-5179., 1963.
13. Crozier, W. D., Atmospheric Electrical Profiles below Three Meters, J. Geophys. Res., 70(12), 2785-2792, 1965.
14. Currie, D. R. and K. S. Kreielsheimer, A Double Field Mill for the Measurement of Potential Gradients in the Atmosphere, J. Atmosph. Terr. Phys., 19, 126-135, 1960.

15. Feynman, R. P., R. B. Leighton and M. Sands, The Feynman Lectures on Physics, Vol. 1, Addison-Wesley Publishing Company, Massachusetts, 1966.
16. Fitzgerald, D. R. and H. R. Byers, Aircraft Observations of Convective Cloud Electrification, Proc. 2nd International Conf. on Atmospheric and Space Electricity, 245-268, 1958.
17. Fitzgerald, D. R. and R. C. Sagalyn, Atmospheric Electricity, Chapter 8, Handbook of Geophysics and Space Environments. Air Force Cambridge Research Laboratories, Massachusetts, 1967.
18. Ford, J. W., Paper at 2nd Wentworth Conf., Unpublished, 1958.
19. Gathman, S. C., The Effects of Local Atmospheric Space Charge on Surface Electric Fields, Trans, Amer. Geophys. Union, 48, 107, 1967.
20. Hatakeyama, H., The Distribution of the Sudden Change of Electric Field on the Earth's Surface due to Lightning Discharge, Proc. 2nd International Conference on Atmospheric and Space Electricity, 289-298, 1958.
21. Hoppel, W. A., The Ions of the Troposphere: their Interactions with Aerosols and the Geoelectric Field, Ph. D. Thesis, The Catholic University of America, Washington, D. C., 1968.
22. Hoppel, W. A., Electrode Effect: Comparison of Theory and Measurement, Proc. 4th International Conf. on the Universal Aspects of Atmospheric Electricity, II. 167-181, 1969.
23. Israel, H., Atmospheric Electricity, I, Israel Program for Scientific Translations, Jerusalem, 1970.
24. Israel, H. in cooperation with H. Dolezalek, Atmospheric Electricity, II., Israel Program for Scientific Translations, Jerusalem, 1973.
25. Israel, H. and H. Dolezalek, On the Problem of Comparing Atmospheric Electric Results, Lectures at the Symposium on Atmospheric Electricity, U G G I Conference, Helsinki, 336, 553, 1960.
26. Israel, H., Problems of Fair-Weather Electricity, Proc. 3rd International Conference on Atmospheric and Space Electricity, 59-67, 1965.
27. Jackson, J. D., Classical Electrodynamics, John Wiley & Sons, Inc., New York, 1962.

28. Kraakevik, J. H., Electrical Conduction and Convection Currents in the Troposphere, Proc. 2nd International Conf. on Atmospheric and Space Electricity, 75-88, 1958.
29. Kuo, H. and A. A. Few, Determination of the Air Electric Current through the Use of a Conducting Hemisphere Pair Suspended in an Electric Field, EOS, Trans. Amer. Geophys. Union., 53(11), 1005, 1972.
30. Mohnen, V. A., Preliminary results on the Formation of Negative Small Ions in the Troposphere, J. Geophys. Res., 75(9), 1717-1721, 1970.
31. Muhleisen, R., The Influence of Water on the Atmospheric Electric Process, Proc. 2nd Int. Conf. on Atmospheric and Space Electricity, 213-222, 1958.
32. Muhleisen, R., Electrode Effect Measurements above the Sea, J. Atmospheric Terrest. Phys., 20, 79-81, 1961.
33. Nolan, J. J., and P. J. Nolan, Atmospheric Electrical Conductivity and the Current from Air to Earth, Proc. Roy. Irish. Acad., 43, 79-93, 1937.
34. Pierce, E. T., Waterfalls, Bathrooms and -perhaps- Supertanker Explosions, Atandard Research Institute Scientific Note, 14, 1970.
35. Serbu, G. P. and E. M. Trent, A Study of the Use of Atmospheric-Electric Measurements in Fog Forecasting, Trans. Amer. Geophys. Union, 39, 1034-1042, 1958.
36. Serbu, G. P., Atmospheric Electricity and Advection Fog Forecasting, Proc. 2nd International Conf. on Atmospheric and Space Electricity, 239-240, 1958.
37. Sharpless, G. T., W. P. Aspinall and W. C. A. Hutchinson, Atmospheric Electricity Observations at a Land Station in Fair Weather, J. Geomag. and Geoelec., 23(3), 335-346, 1971.
38. Smiddy, M. and J. A. Chalmers, The Double Fieldmill, J. Atmosph. Terr. Phys. 12, 206-210, 1958.
39. Smiddy, M. and J. A. Chalmers, Measurements of Space Charge in the Lower Atmosphere Using Double Field Mills, Quart. J. R. Met. Soc., 86, 79-84, 1960.
40. Sten, Wohlers, Boubel and Lowry, Fundamentals of Air Pollution, Academic Press, New York, 1973.
41. Swan, W. F. G., On Certain New Atmospheric-Electric Instruments and Methods, Terr. Magn. Atmos. Elect., 19, 171-185, 1914.

42. Takahashi, T., Measurement of Electric Charge of Cloud Droplets, Drizzle and Raindrops, Reviews of Geophys. and Space Physics, III(4), 903-924, 1973.
43. Uman, M. A., Lightning, Advanced Physics Monograph Series, McGraw-Hill Book Com., New York, 1969.
44. Vonnegut, B. and C. B. Moore, Preliminary Attempts to Influence Convective Electrification in Cumulus Clouds by Introduction of Space Charge into the Lower Atmosphere, Proc. 2nd International Conf. on Atmospheric and Space Electricity, 317-332, 1958.
45. Wait, G. R., Some Experiments Relating to the Electrical Conductivity of the Lower Atmosphere, J. Washington Acad. Sci., 36(10), 321-343, 1946.
46. Weed, M. and P. Kellogg, Strong Electric Field above an Ordinary Rain Cloud, Nature, 249, 134-135, 1974.

END 1-77